BNL- 52502
Formal Report

DYNAMIC RESPONSE OF CANTILEVER RETAINING WALLS

A. S. Veletsos, A. H. Younan and K. Bandyopadhyay

bnl
aui

October 1996

DEPARTMENT OF ADVANCED TECHNOLOGY
BROOKHAVEN NATIONAL LABORATORY, ASSOCIATED UNIVERSITIES, INC.
UPTON, NEW YORK

UNITED STATES DEPARTMENT OF ENERGY
CONTRACT NO. DE-ACO2-76H00016

BNL-52502
UC-406

DYNAMIC RESPONSE OF CANTILEVER RETAINING WALLS

A. S. Veletsos, A. H. Younan and K. Bandyopadhyay

October 1996

Prepared for
OFFICE OF ENVIRONMENTAL RESTORATION AND WASTE MANAGEMENT
DEPARTMENT OF ENERGY, WASHINGTON, D.C.

ABSTRACT

A critical evaluation is made of the response to horizontal ground shaking of flexible cantilever retaining walls that are elastically constrained against rotation at their base. The retained medium is idealized as a uniform, linear, viscoelastic stratum of constant thickness and semiinfinite extent in the horizontal direction. The parameters varied include the flexibilities of the wall and its base, the properties of the retained medium, and the characteristics of the ground motion. In addition to long-period, effectively static excitations, both harmonic base motions and an actual earthquake record are considered. The response quantities examined include the displacements of the wall relative to the moving base, the wall pressures, and the associated shears and bending moments. The method of analysis employed is described only briefly, emphasis being placed on the presentation and interpretation of the comprehensive numerical solutions. It is shown that, for realistic wall flexibilities, the maximum wall forces are significantly lower than those obtained for fixed-based rigid walls and potentially of the same order of magnitude as those computed by the Mononobe-Okabe method.

TABLE OF CONTENTS

LIST OF FIGURES

LIST OF TABLES

Table **Page**

EXECUTIVE SUMMARY

The study reported here is the fifth in a series of investigations of the response to ground shaking of retaining walls and deeply embedded vertical cylindrical structures. The objectives of these studies have been to provide insights into the dynamic responses of these systems and to formulate rational but simple methods for their analysis and design. The previous studies were described in Brookhaven National Laboratory reports 52357, 52372, 52402 and 52444.

Past analyses of the dynamic response of retaining walls may be classified into two groups: (1) elastic analyses, in which the wall is considered to be fixed against both deflection and rotation at the base and the backfill is presumed to respond as a linearly elastic or viscoelastic material; and (2) limit state analyses, in which the wall is considered to displace sufficiently at the base to mobilize the full shearing strength of the backfill.

The wall pressures and associated forces computed by elastic analyses are from 2.5 to over 3 times as large as those determined by limit state analyses, and elastic solutions are generally deemed to be unduly conservative and inappropriate for use in design applications. In a recent contribution by the authors, it has been shown that, for walls that are rigid but elastically constrained against rotation at their base, both the magnitudes and distributions of the dynamic wall pressures and forces are quite sensitive to the flexibility of the base constraint and that, for realistic base flexibilities, these effects may be significantly lower than those computed for non-deflecting, rigid walls. Comparable results also are expected for walls that are themselves flexible.

The purpose of this study is to make a critical evaluation of the magnitude and distribution of the dynamic displacements, pressures and forces induced by horizontal ground shaking in walls that are both flexible and elastically constrained against rotation at their base, and to assess the effects and relative importance of the numerous factors involved. The soil is presumed to act as a uniform viscoelastic stratum of constant thickness and infinite extent in the horizontal direction, and the bases of the wall and soil stratum are presumed to be excited by a space-invariant horizontal motion.

The principal conclusions of the study may be summarized as follows:

1. For the soil-wall system examined, both the magnitudes and distributions of the wall displacements, wall pressures and associated forces induced by horizontal ground shaking are quite sen-

sitive to the flexibilities of the wall and its base. Increasing either flexibility reduces the horizontal extensional stiffness of the retained medium relative to its shearing stiffness, and this reduction decreases the proportion of the soil inertia forces that gets transferred to the wall and, hence, the forces developed in it.

2. For realistic wall flexibilities, the total wall force or base shear is one-half or less of that obtained for a fixed-based, rigid wall, and the corresponding reduction in the overturning base moment is even larger. With the information that has been presented, the precise dependence of these critical forces on the flexibilities of the wall and its base may be evaluated readily.

3. When the dynamic amplification effects of the retained medium are neglected, the magnitude of the total wall force obtained for realistic wall flexibilities by the present method of analysis is in reasonable agreement with that computed by the limit-state, Mononobe-Okabe method which also disregards the dynamic amplifications. Additionally, the effective wall height, which is the height by which the total wall force must be multiplied to obtain the overturning base moment, may well be of the order of 40 percent or less of the actual wall height. These values are in close agreement with the 1/3 value involved in the original M-O method, and substantially smaller than the 60 percent value recommended in the Seed-Whitman modification of the method.

4. For systems excited by earthquake ground motions of the type recorded during the El Centro, California event, the dynamic amplification factor for total wall force for the most unfavorable combination of system parameters is likely to vary from 1.3 for fixed-based, rigid walls to 1.9 for walls of high flexibility. The effective wall height, on the other hand, is insensitive to the ground motion characteristics, and may be taken equal to that obtained for 'statically excited' systems.

5. Even for the 1940 El Centro earthquake motion, the maximum wall displacement relative to the moving base for realistic systems is found to be less than the values of 0.1% to 0.4% of the wall height normally accepted as the minimum required to develop a limit state in the retained material.

6. The comprehensive numerical solutions presented and their analysis provide not only valuable insights into the effects and relative importance of the numerous factors that influence the response of the systems examined, but also a sound framework for assessing the behavior of even more complex soil-wall systems. It is hoped that the information presented will also lead to a greater appreciation than appears to exist at present of the value of elastic methods of analysis for the problem examined.

7. The effects of nonuniformity in the shear modulus of the retained medium and of separation at the wall-medium interface were examined briefly from a static point of view. The dynamic aspects of these issues require further study.

ACKNOWLEDGMENT

This study was carried out under Projects 558223 and 568821 from Brookhaven National Laboratory, Upton, New York. This support is acknowledged gratefully, as are numerous valuable comments received from Dr. Morris Reich.

SECTION 1
INTRODUCTION

Despite the multitude of studies that have been carried out over the years, the dynamic response of cantilever retaining walls is far from being well understood. There is, in particular, a paucity of conclusive information that may be used in design applications.

Past analyses of the dynamic response of such systems may be classified into two groups: (1) elastic analyses, in which the wall is considered to be fixed against both deflection and rotation at the base and the backfill is presumed to respond as a linearly elastic or viscoelastic material; and (2) limit state analyses, in which the wall is considered to displace sufficiently at the base to mobilize the full shearing strength of the backfill.

Representative of the first group of studies are the contributions of Matuo and Ohara (1960), Wood (1973), and Veletsos and Younan (1994a, 1994b), and representative of the second group is the Mononobe-Okabe (M-O) approach (Mononobe and Matuo, 1929; Okabe 1924) and its variants (Seed and Whitman, 1970; Richards and Elms, 1979; Nadim and Whitman, 1983) which have found widespread acceptance in practice (e.g., ATC 1981). More detailed accounts of previous analytical and experimental studies on the subject matter have been presented by Nazarian and Hadjian (1979), Prakash (1981), Whitman (1991), and Veletsos and Younan (1995).

The wall pressures and associated forces computed by elastic analyses are from 2.5 to over 3 times as large as those determined by the M-O approach, and elastic solutions are generally deemed to be unduly conservative and inappropriate for use in design applications. There is, in fact, a widespread mistrust in elastic methods and a corresponding overconfidence in limit-state analyses, such as the venerable M-O method, even for conditions for which the latter method is not applicable. However, excepting some recent exploratory studies (Finn *et al.*, 1989; Siller *et al.*, 1991; Sun and Lin, 1995), the existing elastic solutions are limited to non-deflecting, rigid walls, and do not provide for the important effect of wall flexibility. Furthermore, the limited numerical data presented by Sun and Lin (1995) are believed to be in error.

In a recent contribution by the authors (Veletsos and Younan, 1994b), it has been shown that, for walls that are rigid but elastically constrained against rotation at their base, both the magnitudes and

distributions of the dynamic wall pressures and forces are quite sensitive to the flexibility of the base constraint and that, for realistic base flexibilities, these effects may be significantly lower than those computed for non-deflecting, rigid walls. Comparable results also are expected for walls that are themselves flexible.

The purpose of this study is to make a critical evaluation of the magnitude and distribution of the dynamic displacements, pressures and forces induced by horizontal ground shaking in walls that are both flexible and elastically constrained against rotation at their base, and to assess the effects and relative importance of the numerous factors involved. The soil is presumed to act as a uniform viscoelastic stratum of constant thickness and infinite extent in the horizontal direction, and the bases of the wall and soil stratum are presumed to be excited by a space-invariant horizontal motion. The factors investigated include the characteristics of the ground motion, the properties of the stratum, and the flexibilities of the wall and of the rotational base constraint. Both harmonic and earthquake-induced ground motions are examined. Special attention is paid to the effects of long-period, effectively static excitations. A maximum response for the dynamically excited system is then expressed as the product of the corresponding long-period, static response and an appropriate amplification or deamplification factor. The method of analysis employed is described only briefly, the emphasis being on the presentation and interpretation of the comprehensive numerical solutions.

SECTION 2

SYSTEM CONSIDERED

The system examined is shown in Fig. 2.1(a). It consists of a semiinfinite, uniform layer of viscoelastic material of height H that is free at its upper surface, is bonded to a rigid base, and is retained along one of its vertical boundaries by a uniform, flexible cantilever wall that is elastically constrained against rotation at its base. The bases of both the wall and the soil stratum are presumed to experience a space-invariant horizontal motion, the acceleration of which at any time t is $\ddot{x}_g(t)$ and its maximum value is $\ddot{X}_g$. Material damping for the medium is considered to be of the constant hysteretic type.

The properties of the soil stratum are defined by its mass density ρ, shear modulus of elasticity G, Poisson's ratio ν, and the material damping factor δ, which is considered to be frequency-independent and the same for both shearing and axial deformations. The factor δ is the same as the $\tan\delta$ factor used previously by the senior author and his associates in studies of foundation dynamics (e.g., Veletsos and Verbic, 1973; Veletsos and Dotson, 1988), and twice as large as the factor β employed by others in related studies (e.g., Roesset *et al.*, 1973; Pais and Kausel, 1988). The properties of the wall are defined by its thickness t_w, mass per unit of surface area μ_w, Young's modulus of elasticity E_w, Poisson's ratio ν_w, and material damping factor δ_w which is considered to be the same for both the wall in flexure and the rotational base constraint. The latter factor, like δ, is twice as large as the corresponding percentage of critical damping. The stiffness of the rotational base constraint is denoted by R_θ.

The wall displacements relative to the moving base and the resulting wall pressures and forces for the base-excited system can be shown to be identical to those for the force-excited system displayed in Fig. 2.1(b), for which the base is stationary and the stratum and wall are subjected to uniform lateral body forces of intensity $-\rho\,\ddot{x}_g(t)$ and $-\mu_w\,\ddot{x}_g(t)$, respectively. For excitations with dominant frequencies that are very low compared to the fundamental frequency of the stratum, the action of the force-excited system may be easier to visualize than that of the base-excited system.

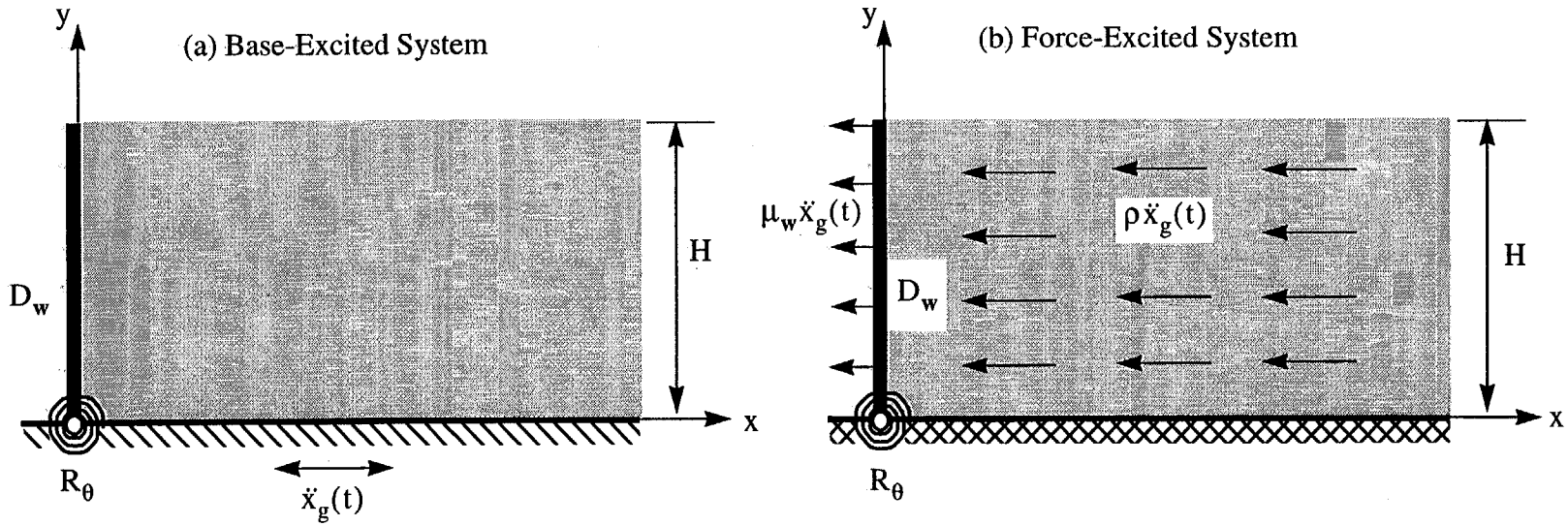

Figure 2.1 Soil-Wall System Investigated

SECTION 3

METHOD OF ANALYSIS

Fundamental to the analysis employed is the assumption that, under the horizontal excitation considered, no vertical normal stresses develop anywhere in the medium, i.e. $\sigma_y = 0$. It is further assumed that there is complete bonding between the wall and the retained medium, and that the horizontal variations of the vertical displacements of the medium are negligible so that the horizontal shearing stresses τ_{xy} can be expressed as $\tau_{xy} = G^*(\partial u/\partial y)$, where u = the horizontal displacement of an arbitrary point of the medium relative to the moving base, $G^* = G(1 + i\delta)$ = the complex-valued shear modulus, and $i = \sqrt{-1}$. The reliability of these assumptions has been confirmed for the limiting case of fixed-based rigid walls (Veletsos and Younan, 1994b) by comparing the results obtained by the present method and Wood's 'exact' solution (1973).

The instantaneous value of the displacement relative to the moving base of an arbitrary point of the wall, $w(\eta, t)$, is expressed as a linear combination of a function that increases linearly from base to top and the natural modes of vibration of a uniform, flexural cantilever beam as

$$w(\eta, t) = \eta H \theta(t) + \sum_{j=1}^{J} \phi_j(\eta)\, q_j(t) \qquad (1)$$

in which $\eta = y/H$ = a dimensionless vertical position coordinate; $\theta(t)$ = the instantaneous value of the base rotation; $\phi_j(\eta)$ = the jth natural mode of vibration of the cantilever beam; $q_j(t)$ = a generalized coordinate defining the degree of participation of $\phi_j(\eta)$ at any time; and J = the total number of modes considered.

The response of the system is evaluated first for a harmonic excitation. The response to an arbitrary ground motion is then determined by Fourier transform techniques.

The equations of motion for the system are obtained by repeated application of Lagrange's equation (Clough and Penzien, 1994). For the evaluation of the generalized forces, the natural modes of vibration of the cantilever beam $\phi_j(\eta)$ are expressed as linear combinations of the corresponding modes of the retained medium when the latter is considered to act as an unconstrained cantilever shear-beam, i.e. as

$$\phi_j(\eta) = \sum_{n=1}^{N} c_n \psi_n(\eta) = \sum_{n=1}^{N} c_n \sin\left[\frac{(2n-1)\pi}{2}\eta\right] \tag{2}$$

where c_n = dimensionless participation factors defined by appropriate integrals of ϕ_j and ψ_n; n = the order of the shear-beam mode under consideration; and N = a sufficiently large integer. The details of the method of analysis for a system involving a fixed-based cantilever wall will be described elsewhere. The equations governing the response of the more general system examined here are summarized in the Appendix.

3.1 Problem Parameters

The primary parameters governing the response of the system are the relative flexibility of the wall and retained medium, defined by

$$d_w = \frac{GH^3}{D_w} \tag{3}$$

and the relative flexibility of the rotational base constraint and retained medium, defined by

$$d_\theta = \frac{GH^2}{R_\theta} \tag{4}$$

The symbol D_w in (3) represents the flexural rigidity per unit of length of the wall, given by

$$D_w = \frac{E_w t_w^3}{12(1-\nu_w^2)} \tag{5}$$

Also affecting the response are the characteristics of the base motion. For a harmonic excitation, the response is controlled by the frequency ratio ω/ω_1, where ω = the circular frequency of the base motion and of the resulting steady-state response, and ω_1 = the fundamental circular frequency of the stratum when it is considered to act as an unconstrained, vertical cantilever shear-beam. For an arbitrary transient excitation, the relevant stratum property is its fundamental cyclic frequency $f_1 = \omega_1/2\pi$, or its corresponding period $T_1 = 1/f_1 = 2\pi/\omega_1$. Additional parameters are Poisson's ratio and damping factor for the soil, ν and δ, the material damping factor for the wall δ_w, and the ratio of mass densities for the wall and the retained medium $\mu_w/\rho H$.

For the solutions presented in the following sections, the wall is considered to be massless (i.e., $\mu_w = 0$); Poisson's ratio for the soil is taken as $\nu = 1/3$; and the damping factors for the soil and wall are taken as $\delta = 0.1$ and $\delta_w = 0.04$, respectively (i.e., as 5% and 2% of critical damping). The relative flexibility factors d_w and d_θ are varied over wide ranges, and so is the frequency ratio ω/ω_1 for harmonic motions, and the fundamental period of vibration of the stratum T_1 for the earthquake ground motion.

SECTION 4

STATIC RESPONSE

It is desirable to begin by examining the responses obtained for excitations the dominant frequencies of which are extremely small compared to the fundamental frequency of the soil-wall system (i.e., for values of $\omega/\omega_1 \rightarrow 0$ or $f_1 \rightarrow \infty$). Such excitations and the resulting effects are referred to as 'static' and are identified with the subscript st. This term should not be confused with that normally used to represent the effects of gravity forces. In the equivalent, force-excited version of the problem referred to previously, the static excitation is represented by horizontal body forces of intensity $-\rho \ddot{X}_g$ for the retained medium and of $-\mu_w \ddot{X}_g$ for the wall. The maximum value of a dynamic effect for an arbitrary transient excitation is then expressed as the product of the corresponding static effect and an appropriate amplification or deamplification factor.

4.1 Wall Pressures

The heightwise variations of the 'static' wall pressures $\sigma_{st}(\eta)$ are displayed in Fig. 4.1 for systems with different flexibility factors d_w and d_θ. Pressures are considered to be positive when they induce compression on the wall. The plots in part (a) of the figure are for fixed-based walls with different values of d_w, whereas those in part (b) are for rotationally constrained rigid walls with different values of d_θ. The walls in these and all solutions that follow are presumed to be massless, and Poisson's ratio for the retained medium is taken as $\nu = 1/3$.

As might be expected, the wall pressures decrease with increasing d_w or d_θ, the reductions being quite substantial even for small values of the flexibility factors. Increasing the flexibility of the wall or its base reduces the horizontal extensional stiffness of the medium relative to its shearing stiffness, and this reduction, in turn, increases the proportion of the inertia forces transmitted by horizontal shearing action to the base and decreases the proportion transmitted to the wall.

The flexibilities of the wall and its base also affect significantly the distribution of the wall pressures. For fixed-based rigid walls ($d_w = d_\theta = 0$), the pressures increase almost as a quarter-sine from zero at the base to a maximum at the top, whereas for the flexible walls, there is generally a sharp change in magnitude and a reversal in the sign of the pressure at the top. It follows that, whereas the pressure distribution for the fixed-based rigid wall is dominated by the contribution of the fundamental mode of vibration of the soil stratum, the distributions for the flexible walls are affected significantly by the

higher modes.

4.2 Wall Forces

Figure 4.2 shows the heightwise distributions of the static shear per unit of wall length, $V_{st}(\eta)$, and Fig. 4.3 shows the distributions of the corresponding bending moment, $M_{st}(\eta)$. As before, the plots in parts (a) of the figures are for fixed-based, flexible walls, whereas those in part (b) are for walls that are rigid and elastically constrained against rotation at the base. These forces are computed by appropriate integrations of the wall pressures $\sigma_{st}(\eta)$. Shears are normalized with respect to $\rho\ddot{X}_g H^2$ and moments with respect to $\rho\ddot{X}_g H^3$.

As would be expected from the information on wall pressures presented in Fig. 4.1, increasing the flexibility of either the wall or of the rotational base constraint decreases the magnitude of the wall forces, the reductions being considerably larger for bending moments than for shears and, in both instances, quite substantial even for relatively small values of d_w or d_θ.

In Fig. 4.4, the normalized static values of the base shear and base moment, $(V_b)_{st}/\rho\ddot{X}_g H^2$ and $(M_b)_{st}/\rho\ddot{X}_g H^3$, are plotted as a function of the wall flexibility factor d_w for several values of the base flexibility factor d_θ. For fixed-based rigid walls ($d_w = d_\theta = 0$), the base shear and base moment have the well established values of $0.940\rho\ddot{X}_g H^2$ and $0.563\rho\ddot{X}_g H^3$, respectively (Veletsos and Younan, 1994b). The base shear is effectively equal to the inertia force acting on a rectangular body of soil of width 0.94H and height H, and the base moment is equal to the product of the total wall force or base shear and a height $h = 0.6H$, which will be referred to as the effective height. Incidentally, the latter value is close to the $2/\pi$ value corresponding to a pressure distribution that increases as a quarter-sine from base to top. The latter distribution is obtained on assuming that the soil responds in its fundamental mode of vibration. Selected values of the normalized base shear are also listed in part (a) of Table 4.1.

As an indication of the effect of wall flexibility on the response of a representative practical system, it is noted that for the relatively low values of $d_w = 5$ and $d_\theta = 1$, the base shear $(V_b)_{st} = 0.496\rho\ddot{X}_g H^2$. This value is only 53% of that obtained for a fixed-based rigid wall and 32% higher than the $0.375\rho\ddot{X}_g H^2$ value computed by the limit-state, M-O method of analysis (Seed and Whitman, 1970). For higher but still realistic values of the flexibility factors d_w and d_θ, the agreement in the results obtained by the present analysis and the M-O method is even better.

The values of the effective wall height h for systems with different combinations of the flexibility factors d_w and d_θ are plotted in Fig. 4.5 normalized with respect to the actual height H. Selected values are also listed in part (b) of Table 4.1. Note that for the values of $d_w = 5$ and $d_\theta = 1$ considered in the example referred to above, $h = 0.403H$, which is only 21% higher than the H/3 value associated with the original M-O method of analysis and significantly lower than the 0.6H value

recommended in the Seed-Whitman modification of the method (1970). For larger values of d_w and d_θ, the value of h, as demonstrated in Fig. 4.5, may well be less than H/3. Similar low values of h/H have also been determined experimentally in the studies of rocking walls reported by Andersen *et al.* (1987) (see also Whitman, 1990).

While the close agreement in the results obtained for the example considered by the present method and the M-O method constitutes no proof of the validity of either approach, it does demonstrate that the analysis presented leads to results that are in the range of those deemed by many to be appropriate for design purposes, and that elastic methods deserve much greater credit and attention than they have been accorded so far. It should be added that in the evaluation of $(V_b)_{st}$ no provision has been made for the dynamic amplification effects of the retained medium. However, the same is also true of the corresponding force computed by the M-O approach.

4.3 Wall Displacements

It is also desirable to examine the magnitudes and distributions of the relative wall displacements $w_{st}(\eta)$. Considered to be positive when directed away from the retained medium, these displacements are shown in Fig. 4.6, where the plots on the left refer to fixed-based flexible walls, and those on the right to elastically constrained rigid walls. As before, the walls are presumed to be massless, and Poisson's ratio for the soil $\nu = 1/3$. The results are normalized with respect to $\ddot{X}_g H^2/v_s^2$, where $v_s = \sqrt{G/\rho}$ = the shear-wave velocity of the soil medium.

An increase in either wall or base flexibility naturally increases the wall displacements, the percentage increases being largest for the smaller values of the flexibility factors d_w and d_θ. The flexibility of the wall itself also affects the configuration of the resulting displacements. Included for purposes of comparison in dashed lines are the configurations computed on the assumption that the soil stratum acts as an unconstrained cantilever shear-beam. Note that, for large values of d_w and d_θ, the wall displacements tend to those obtained for the shear-beam. Some of these trends can more clearly be seen in Fig. 4.7, in which the normalized values of the maximum or top wall displacement relative to the moving base, $(w_{st})_{max} = w_{st}(1)$, are plotted as a function of the wall flexibility factor d_w for several values of the base flexibility factor d_θ.

It is generally accepted (Clough and Duncan, 1990) that the initiation of a failure plane or the development of a limit state in the retained material requires wall displacements of the order of 0.1% to 0.4% of the wall height. To assess the applicability of the elastic solutions presented here, it is desirable to compare the predictions of the present analysis with the above-referenced values. To this end, consider a system for which the wall flexibility factor has the moderately high value of $d_w = 20$. For typical concrete walls, with $E_w = 3 \times 10^6$ psi, $\nu_w = 0.17$ and $H/t_w = 10$, this value corresponds to a soil with a shear wave velocity $v_s = 150$ m/sec (492 ft/sec). The normalized values of the maximum relative wall displacement in this case are in the range of 0.454 to 0.505. Using the

average value of 0.48, the displacement ratio $w_{st}(1)/H$ for a wall of height $H = 5$ m (16.4 ft) and a ground motion with a peak acceleration $\ddot{X}_g = 0.3g$ turns out to be

$$\frac{w_{st}(1)}{H} = 0.48 \frac{\ddot{X}_g H}{v_s^2} = 0.48 \frac{(0.3 \times 9.81) \times 5}{150^2} = 0.031\% \qquad (6)$$

Even with a dynamic amplification factor of 2.2, which as shown later represents an upper bound for realistic soils and an intense earthquake ground motion, the maximum value of the displacement ratio will be lower than the 0.1% to 0.4% range referred to above. For less intense ground motions and walls that are stiffer relative to the retained soil, this ratio would be even lower.

Table 4.1: Normalized values of static base shear $(V_b)_{st}$ and effective wall height h for different wall and base flexibilities ($\nu = 1/3$, $\mu_w = 0$).

d_w	$d_\theta = 0$	$d_\theta = 1$	$d_\theta = 2$	$d_\theta = 3$	$d_\theta = 4$	$d_\theta = 5$
			(a) Values of $(V_b)_{st}/\rho \ddot{X}_g H^2$			
0	0.940	0.566	0.437	0.371	0.331	0.305
0.5	0.883	0.556	0.434	0.370	0.331	0.305
1.0	0.838	0.547	0.431	0.369	0.331	0.304
2.0	0.770	0.531	0.426	0.367	0.330	0.304
3.0	0.720	0.517	0.421	0.366	0.329	0.303
4.0	0.683	0.506	0.417	0.364	0.328	0.303
5.0	0.653	0.496	0.413	0.362	0.327	0.302
6.0	0.628	0.487	0.409	0.360	0.326	0.301
8.0	0.590	0.471	0.402	0.356	0.324	0.299
10.0	0.561	0.458	0.395	0.352	0.321	0.298
15.0	0.510	0.433	0.380	0.343	0.315	0.293
20.0	0.475	0.413	0.368	0.335	0.309	0.288
30.0	0.429	0.382	0.347	0.319	0.297	0.279
40.0	0.397	0.360	0.330	0.307	0.287	0.270
			(b) Values of h/H			
0	0.599	0.512	0.447	0.396	0.356	0.323
0.5	0.575	0.496	0.436	0.389	0.351	0.320
1.0	0.553	0.481	0.426	0.382	0.346	0.316
2.0	0.517	0.456	0.408	0.369	0.337	0.310
3.0	0.488	0.436	0.393	0.359	0.329	0.305
4.0	0.464	0.418	0.381	0.349	0.323	0.300
5.0	0.444	0.403	0.369	0.341	0.316	0.295
6.0	0.426	0.390	0.360	0.333	0.311	0.291
8.0	0.398	0.368	0.343	0.321	0.301	0.284
10.0	0.376	0.351	0.329	0.310	0.293	0.278
15.0	0.337	0.319	0.304	0.290	0.277	0.265
20.0	0.311	0.298	0.286	0.275	0.265	0.255
30.0	0.278	0.270	0.262	0.254	0.247	0.240
40.0	0.257	0.251	0.245	0.240	0.234	0.229

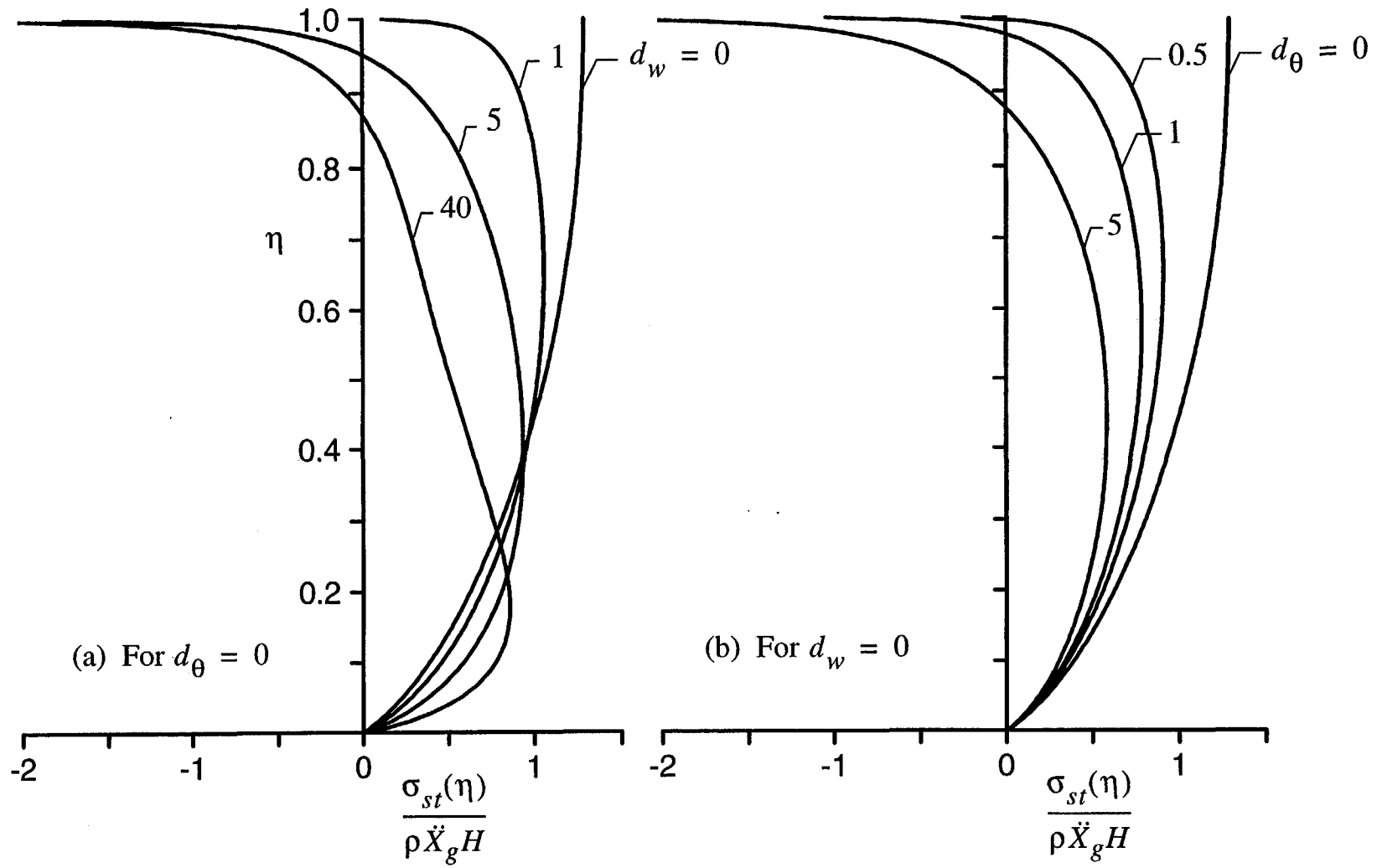

Fig. 4.1 Distributions of Wall Pressure for Statically Excited Systems with Different Wall and Base Flexibilities ($\mu_w = 0$, $\nu = 1/3$).

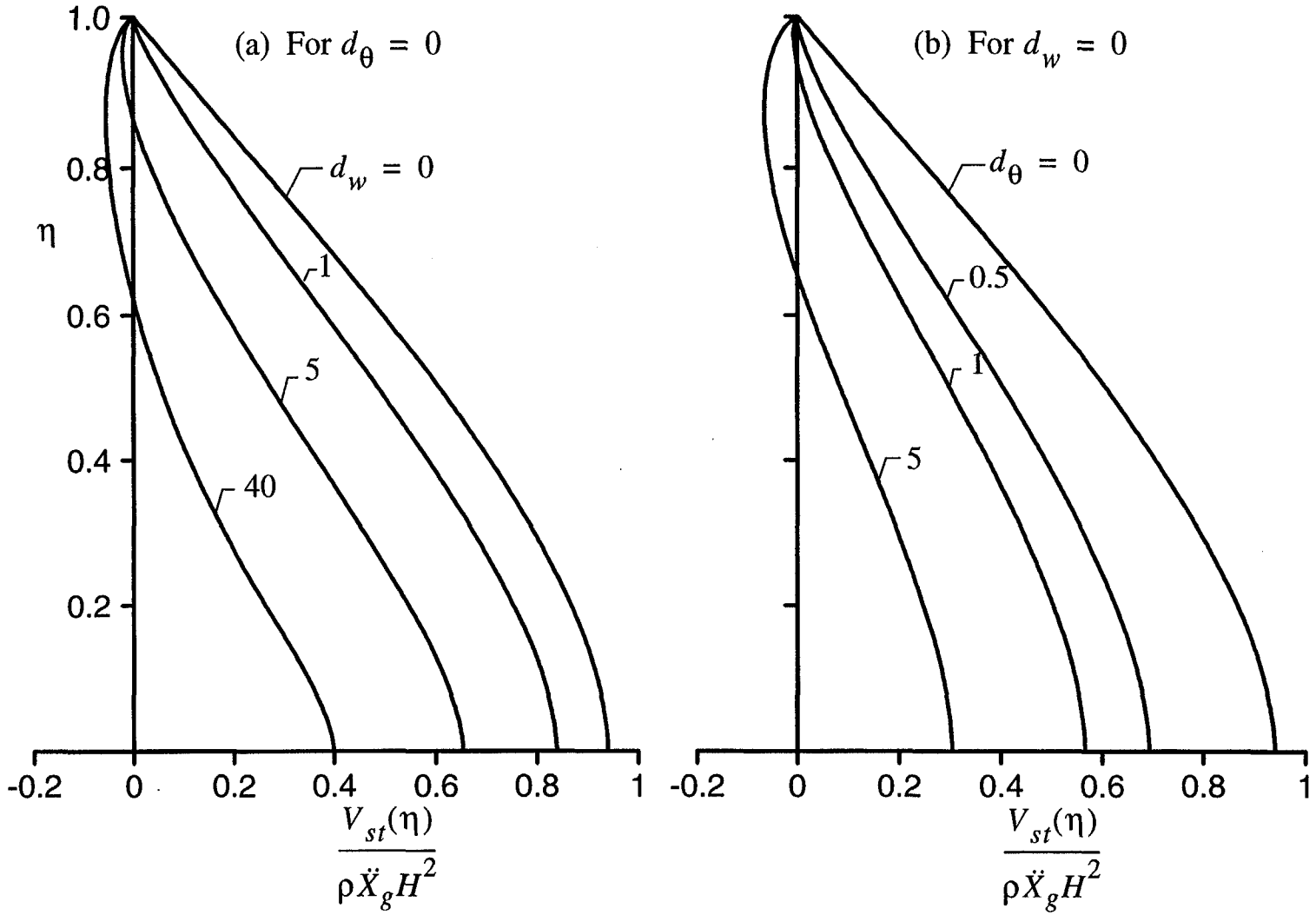

Fig. 4.2 Distributions of Shear in Wall of Statically Excited Systems with Different Wall and Base Flexibilities ($\mu_w = 0$, $\nu = 1/3$).

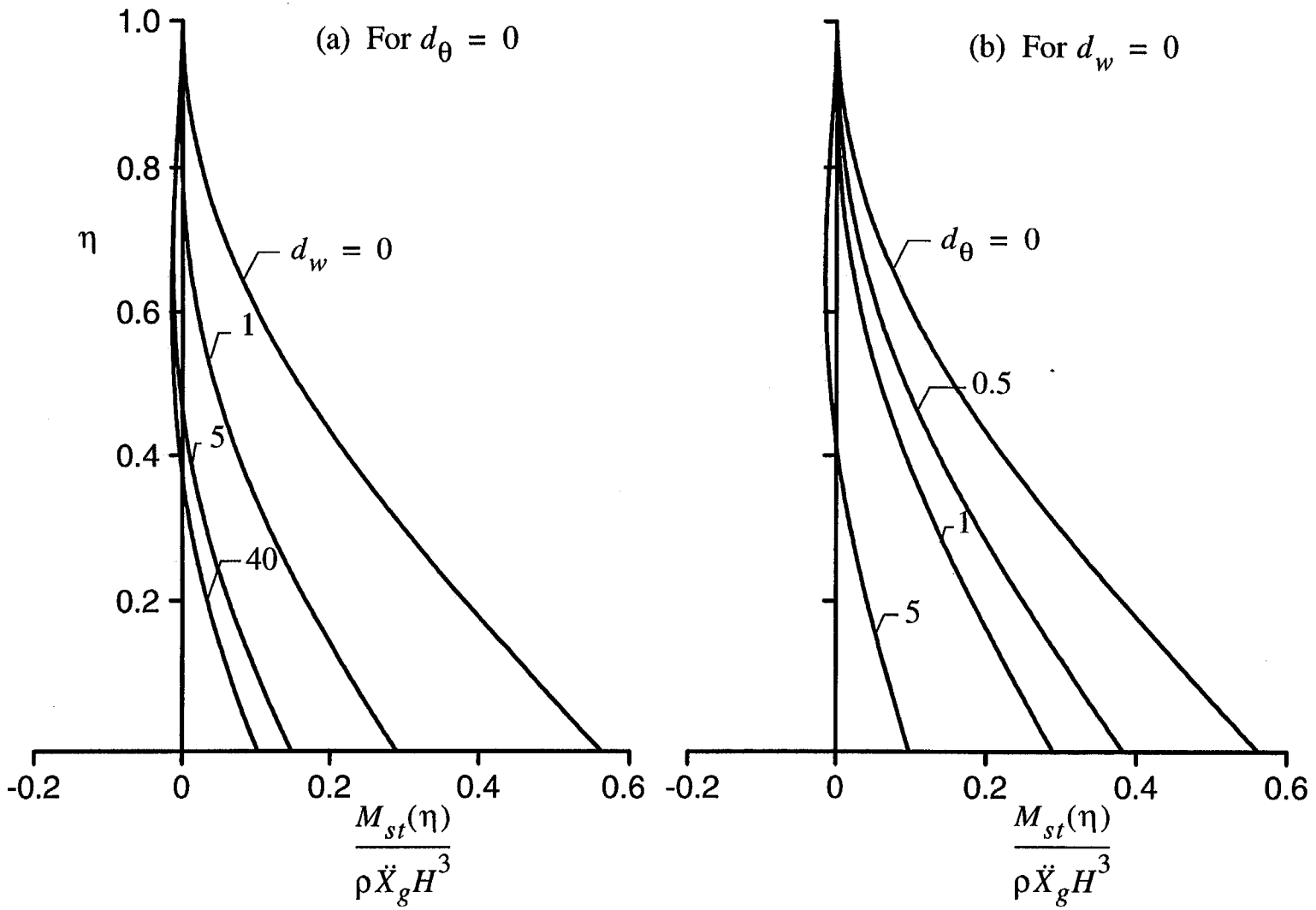

Fig. 4.4 Distributions of Bending Moment in Wall of Statically Excited Systems with Different Wall and Base Flexibilities ($\mu_w = 0$, $\nu = 1/3$).

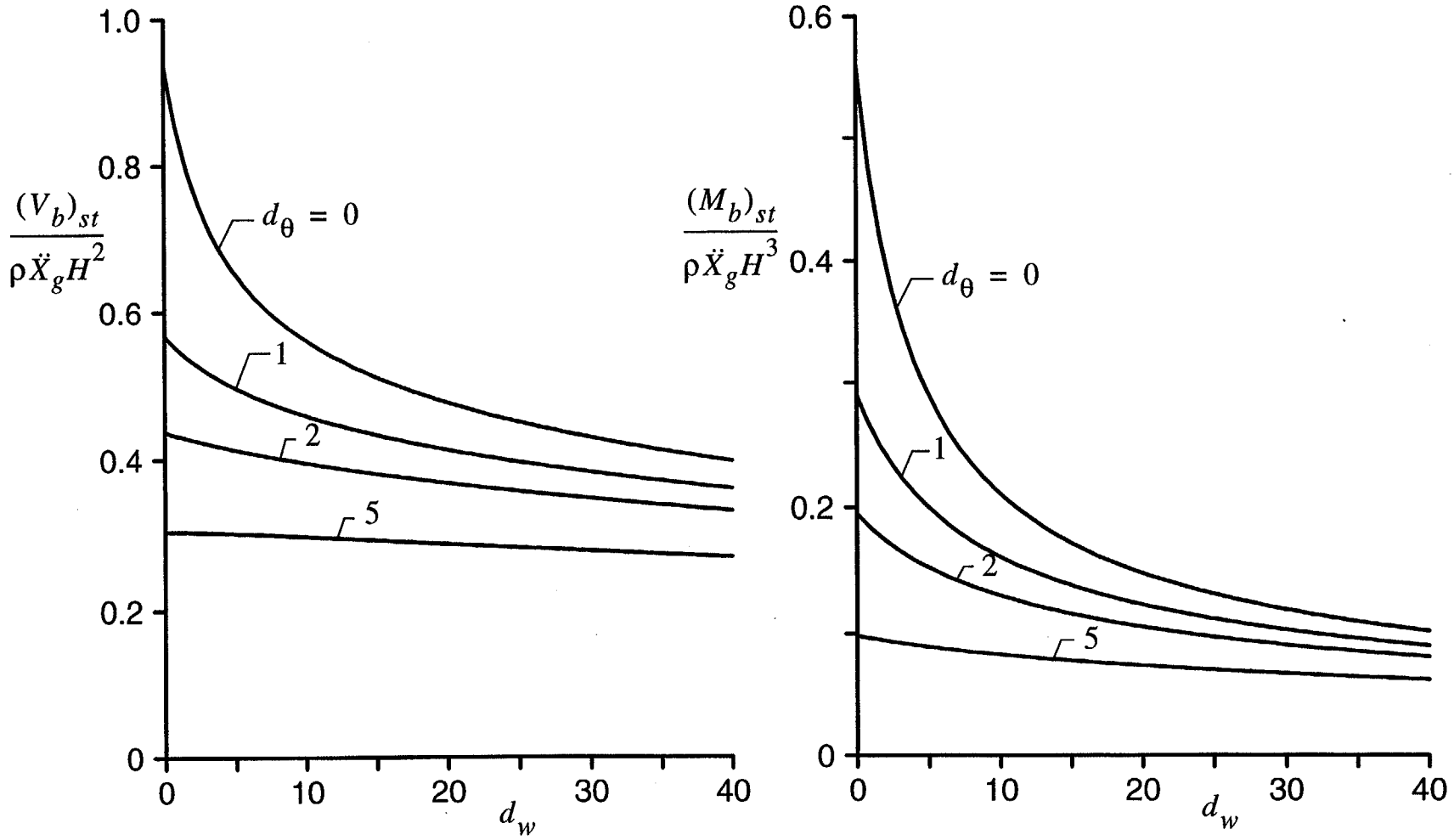

Fig. 4.4 Normalized Values of Base Shear and Moment in Wall of Statically Excited Systems with Different Wall and Base Flexibilities ($\mu_w = 0$, $\nu = 1/3$).

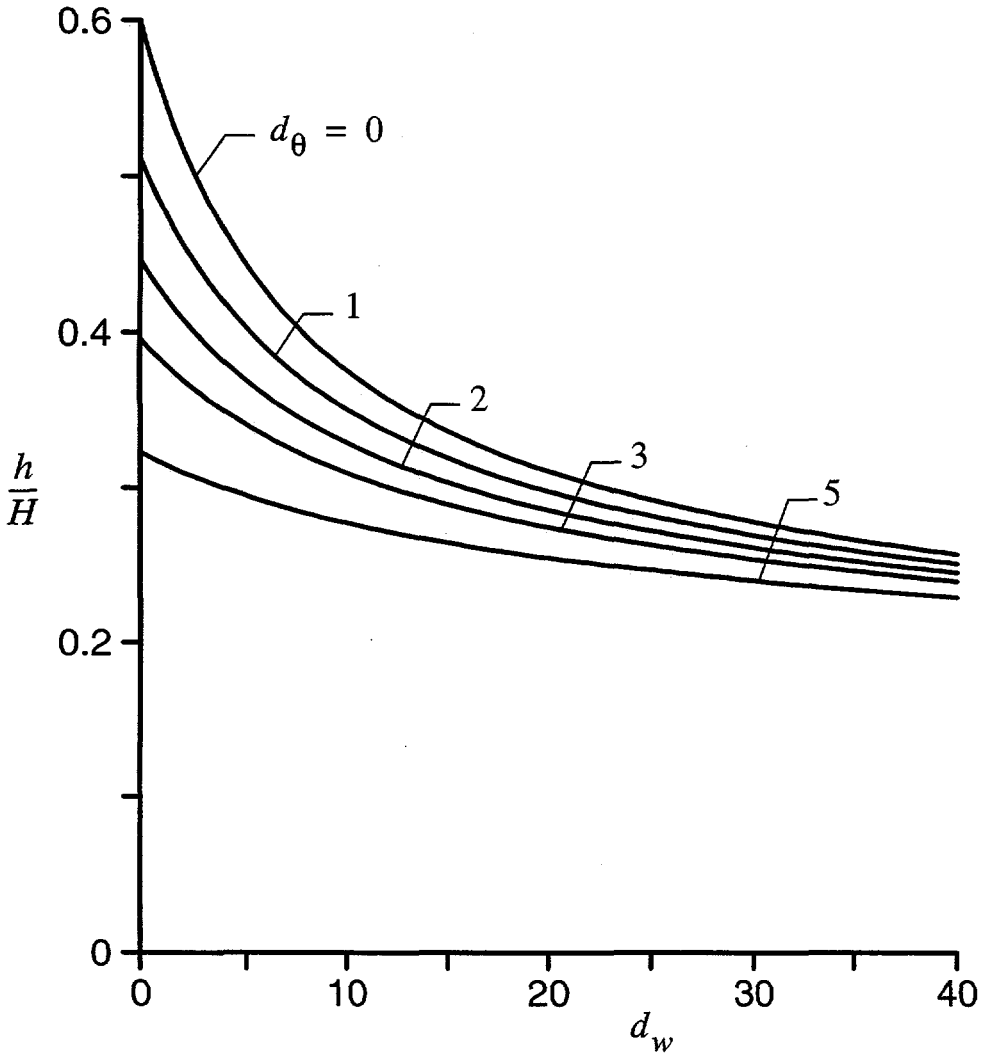

Fig. 4.5 Normalized Effective Heights for Statically Excited Systems with Different Wall and Base Flexibilities ($\mu_w = 0$, $\nu = 1/3$).

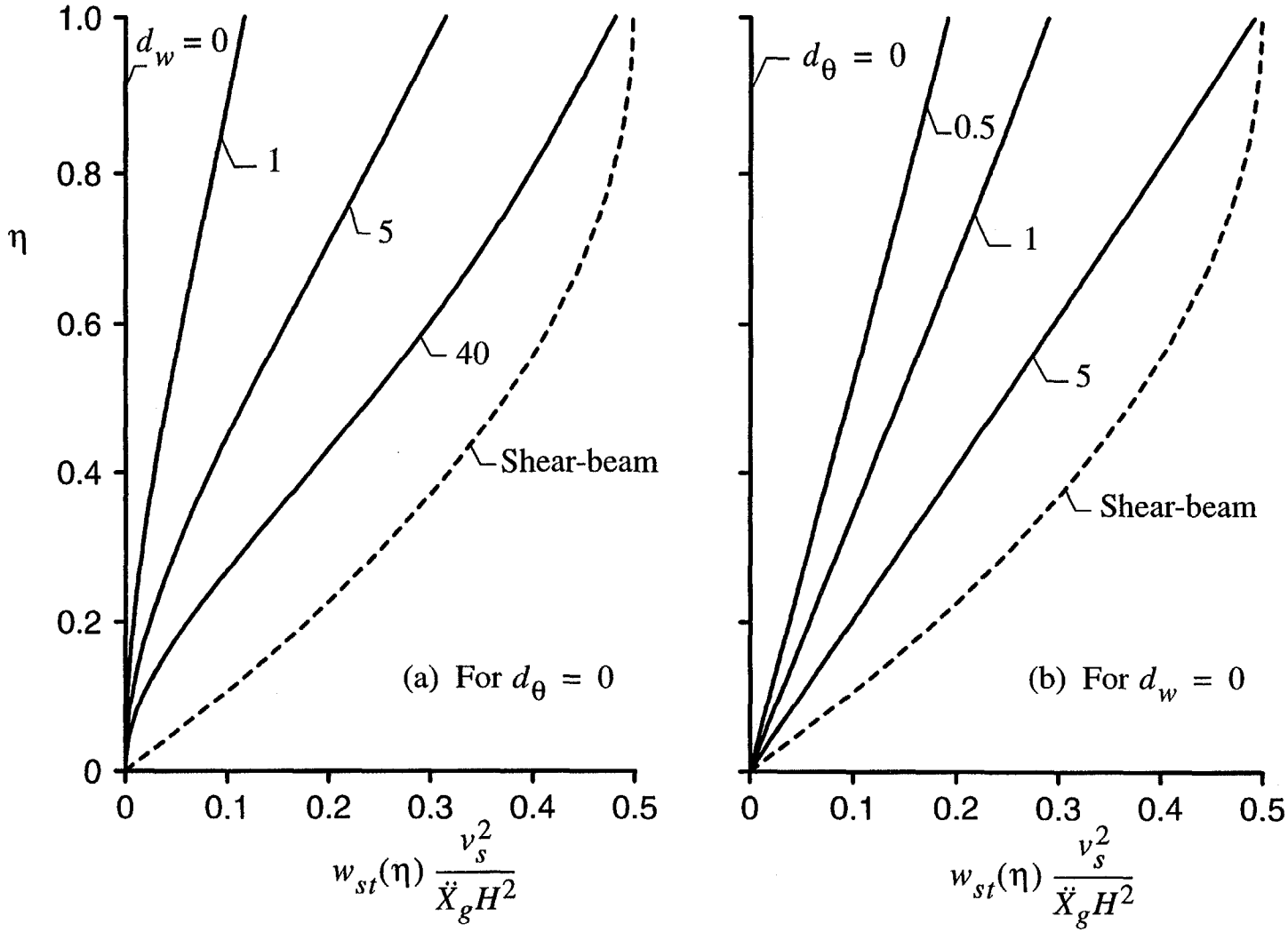

Fig. 4.6 Distributions of Wall Displacement Relative to Base for Statically Excited Systems with Different Wall and Base Flexibilities ($\mu_w = 0$, $\nu = 1/3$).

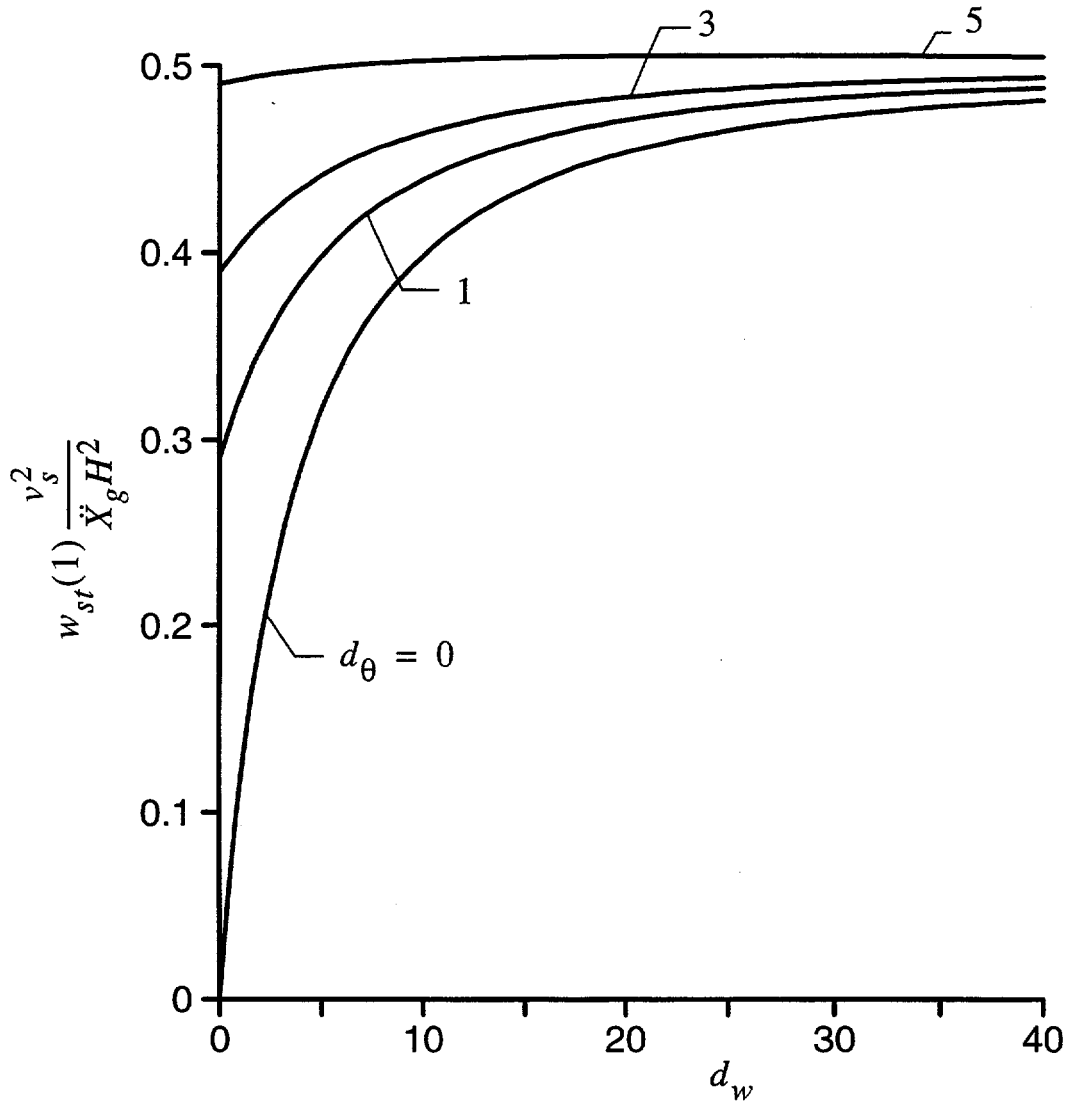

Fig. 4.7 Normalized Top Wall Displacements Relative to Base for Statically Excited Systems with Different Wall and Base Flexibilities ($\mu_w = 0$, $\nu = 1/3$).

SECTION 5

HARMONIC RESPONSE

For the data presented so far, the dominant period of the excitation was considered to be long compared to the natural period of the retained material. In this section, the steady-state response of the system to a harmonic excitation of an arbitrary frequency is examined.

In Fig. 5.1, the amplification factor for base shear in the wall, defined as the ratio of the maximum dynamic to the corresponding static values of the shear, is plotted as a function of the frequency ratio ω/ω_1 for several combinations of the flexibility factors d_w and d_θ. As before, the plots on the left are for fixed-based flexible walls, while those on the right are for rigid walls that are elastically constrained against rotation at the base. In all cases, the walls are presumed to be massless and to have a damping factor $\delta_w = 0.04$ (or 2% of the critical damping), and Poisson's ratio and the damping factor for the retained medium are taken as $\nu = 1/3$ and $\delta = 0.1$.

It is observed that (1) the peak or resonant values of the amplification factors occur at exciting frequencies equal to the natural frequencies of the stratum, i.e., for $\omega/\omega_1 = 1, 3, 5, \ldots$; (2) the absolute maximum amplification factors are attained at the fundamental frequency of the stratum; and (3) the latter factors are quite sensitive to the relative flexibility factors d_w and d_θ. For a fixed-based rigid wall ($d_w = d_\theta = 0$), it is well known (Arias *et al.*, 1981; Veletsos and Younan, 1994a) that the absolute maximum amplification factor for base shear is $1/\sqrt{\delta}$, or 3.16 for the value of $\delta = 0.1$ considered. By contrast, for flexible walls, this factor is substantially larger due to the reduced capacity of such walls to reflect and dissipate by radiation the waves impinging on them. As d_w or d_θ tends to infinity, the soil-wall system tends to respond as an unconstrained cantilever shear-beam, and the absolute maximum amplification factor tends to $1/\delta = 10$, the value applicable to a viscously damped single-degree-of-freedom oscillator.

In Fig. 5.2, the absolute maximum amplification factors for base shear and top displacement of the wall relative to the moving base are plotted as a function of the wall flexibility factor d_w for fixed values of the base flexibility factor d_θ. It is observed that the amplification factors for base shear are somewhat lower than those for displacement. This is attributed to the fact that the static values of the base shear are influenced to a greater extent than those of displacement by the higher modes of vibration.

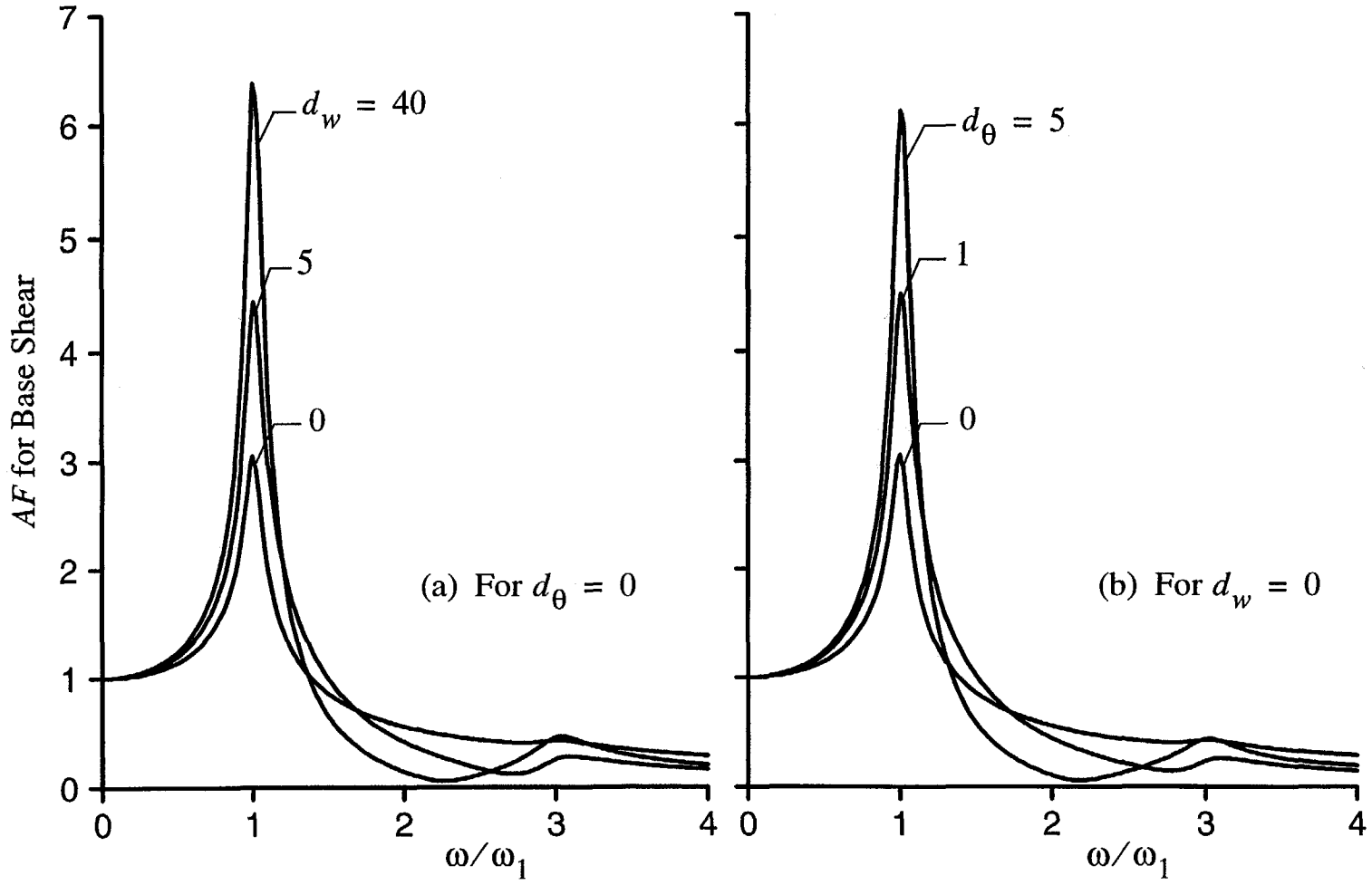

Fig. 5.1 Amplification Factors for Base Shear in Wall of Harmonically Excited Systems with Different Wall and Base Flexibilities ($\nu = 1/3$, $\delta = 0.1$, $\mu_w = 0$, $\delta_w = 0.04$).

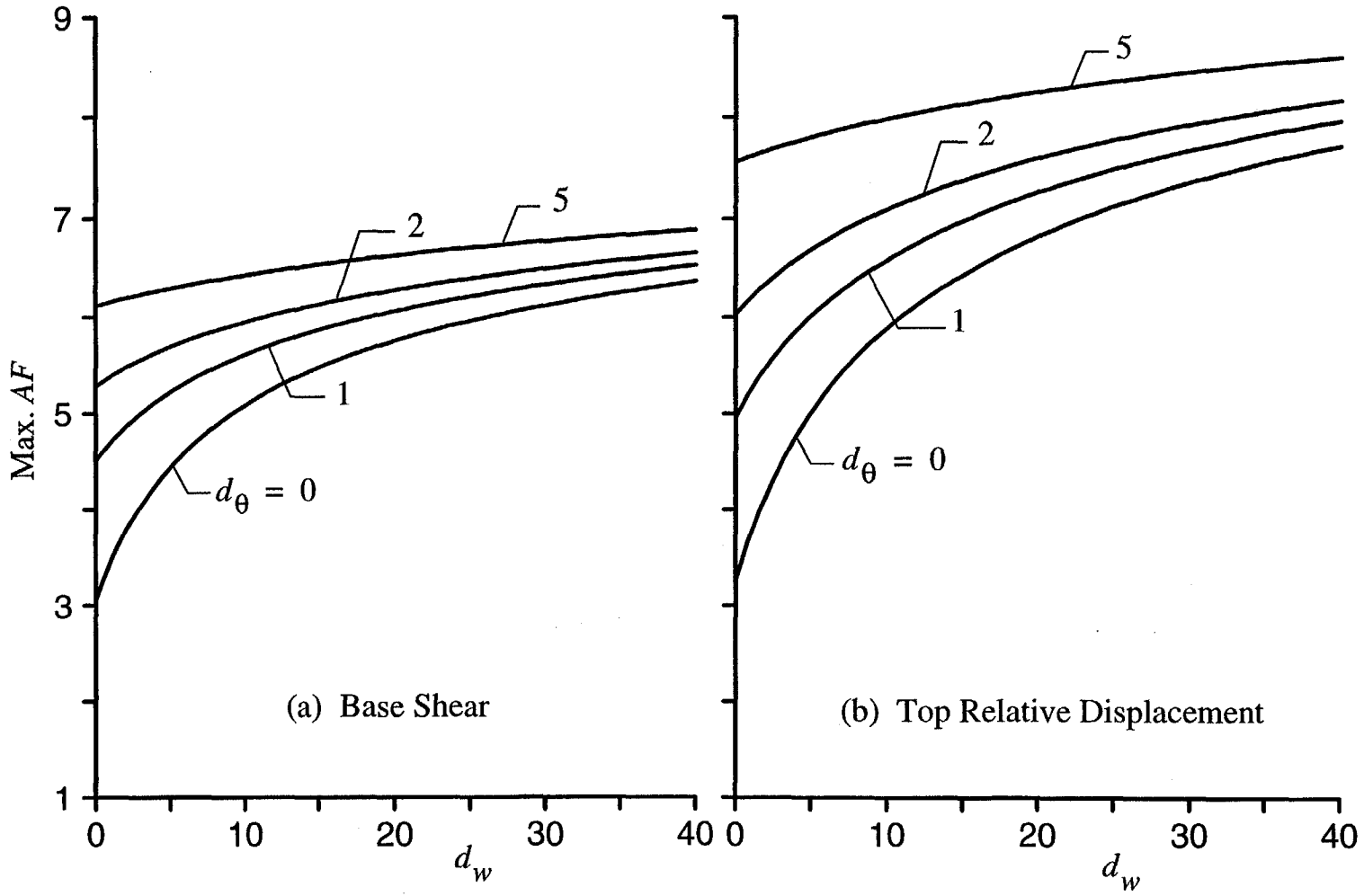

Fig. 5.2 Maximum Amplification Factors for Base Shear and Top Displacement Relative to Base of Harmonically Excited Systems with Different Wall and Base Flexibilities ($\nu = 1/3$, $\delta = 0.1$, $\mu_w = 0$, $\delta_w = 0.04$).

SECTION 6

TRANSIENT RESPONSE

Figure 6.1 shows the amplification factors for maximum base shear in the walls of systems subjected to the first 6.3 sec of the N-S component of the 1940 El Centro, California earthquake ground motion record, the peak acceleration of which $\ddot{X}_g = 0.312g$. As before, the walls in these solutions are presumed to be massless, Poisson's ratio for the retained medium is taken as $\nu = 1/3$, and the damping factors for the wall and soil are taken as $\delta_w = 0.04$ and $\delta = 0.10$ (or 2% and 5% of critical damping, respectively). Both fixed-based flexible walls and elastically constrained rigid walls are considered. The results are plotted as a function of $T_1 = 4H/v_s$, the fundamental period of the soil stratum when it is considered to respond as an unconstrained cantilever shear-beam. As a measure of the values of T_1 that may be encountered in practice, it is noted that for values of v_s between 75 and 300 m/sec (246 and 984 ft/sec) and values of H between 3 and 15 m (9.84 and 49.21 ft), the value of T_1 falls in the range of 0.04 to 0.8 sec.

The plots in Fig. 6.1 are similar to, but by no means the same as, the normalized response spectra for similarly excited, viscously damped single-degree-of-freedom systems. Specifically, for low-natural-period, stiff strata, the amplification factor is unity. With increasing T_1 or increasing flexibility of the stratum, the amplification factors increase, and after attaining nearly horizontal plateaus, they reach values that may be substantially less than unity. In all cases, the amplification factors for the flexible walls are substantially higher than for the corresponding rigid walls. A larger amplification factor, however, does not necessarily imply a higher response level. This can more clearly be seen in Fig. 6.2, in which the base shears for the systems examined in Fig. 6.1 are replotted normalized with respect to the common factor $\rho\ddot{X}_g H^2$.

In part (a) of Fig. 6.3, the amplification factors for base shear in the period range from $T_1 = 0.1$ to 0.5 sec for the conditions considered in Fig. 6.1 are plotted as a function of the flexibility factor d_w for fixed values of d_θ. The period range considered corresponds to the highly amplified, nearly horizontal region of the plots in Fig. 6.1 and 6.2. Also shown in part (b) of Fig. 6.3 are the corresponding factors for top relative wall displacement. It is observed that the factors for base shear range from 1.32 to 1.93, whereas those for top displacement range from 1.39 to 2.38. It should be recalled that these results are for a medium with a damping factor $\delta = 0.10$. An increase in damping will naturally further reduce the amplification factors.

The normalized values of the effective wall heights h for the seismically excited systems are finally plotted in Fig. 6.4 as a function of the fundamental period of the stratum T_1. These heights are relatively insensitive to variations in T_1, and may, for all practical purposes, be taken equal to those reported for the corresponding statically excited systems in Fig. 4.5 and part (b) of Table 4.1.

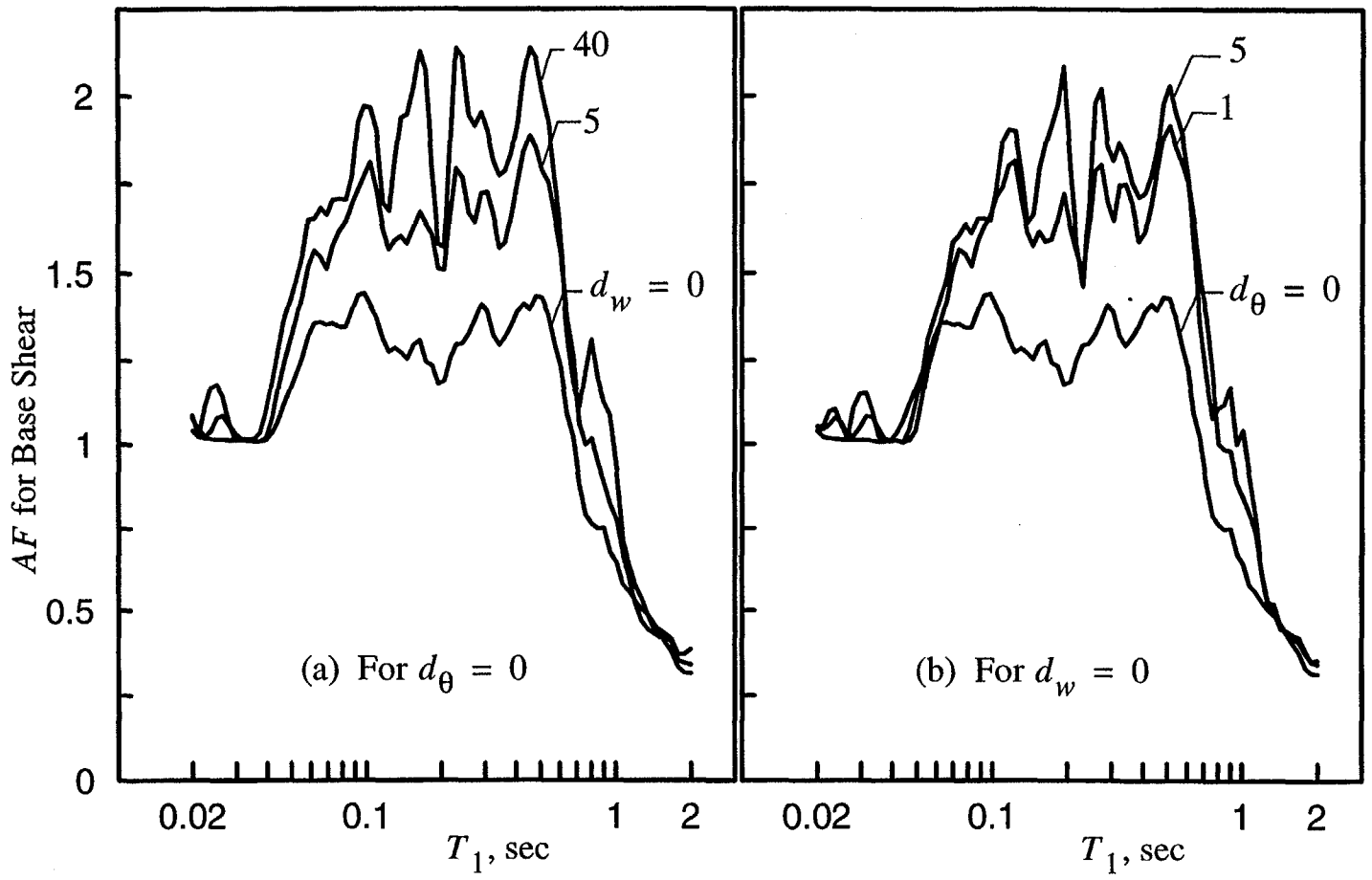

Fig. 6.1 Amplification Factors for Base Shear in Wall of Systems with Different Wall and Base Flexibilities Subjected to El Centro Earthquake Record ($\nu = 1/3$, $\delta = 0.1$, $\mu_w = 0$, $\delta_w = 0.04$).

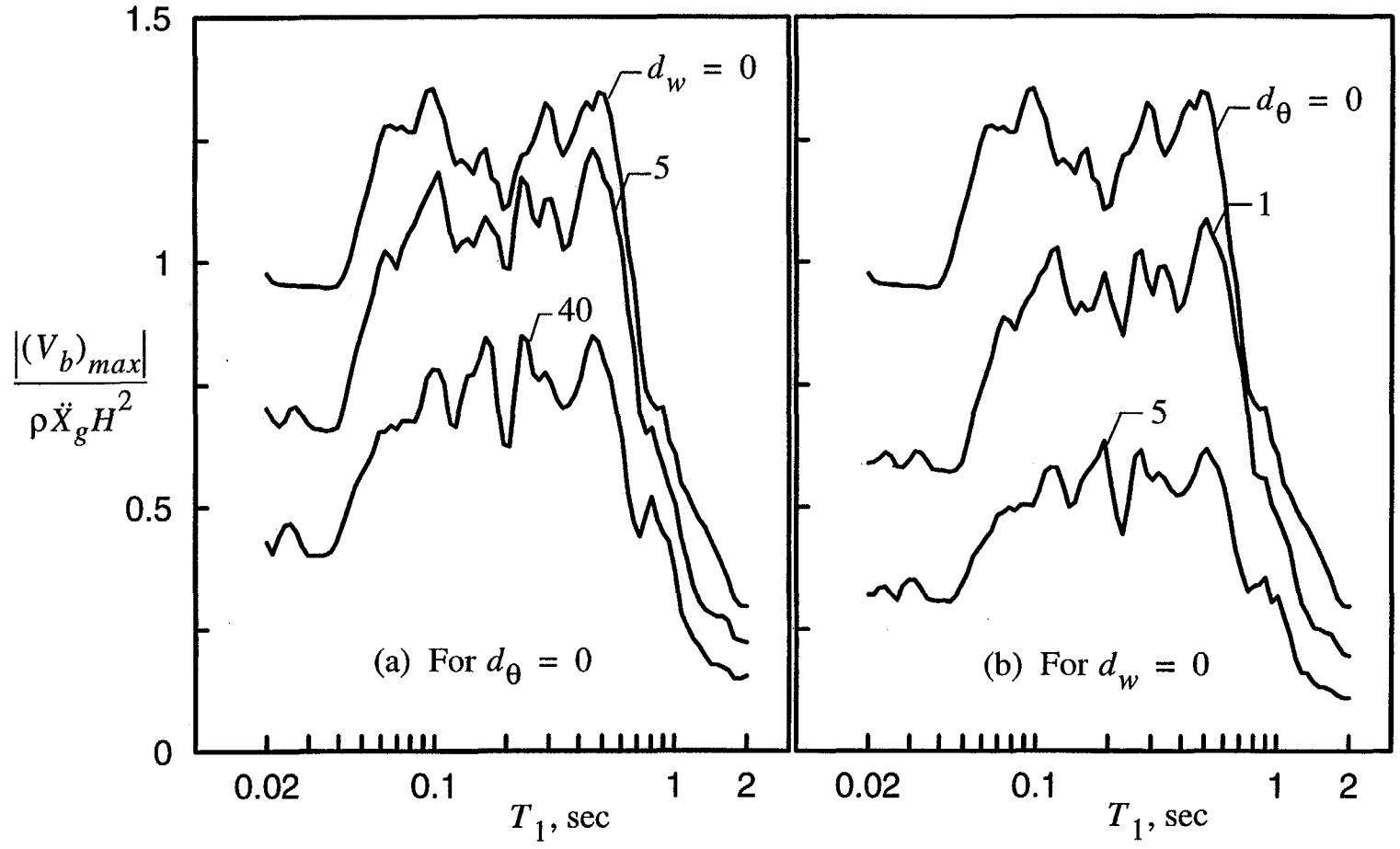

Fig. 6.2 Normalized Values of Maximum Base Shear in Wall of Systems with Different Wall and Base Flexibilities Subjected to El Centro Earthquake Record ($\nu = 1/3$, $\delta = 0.1$, $\mu_w = 0$, $\delta_w = 0.04$).

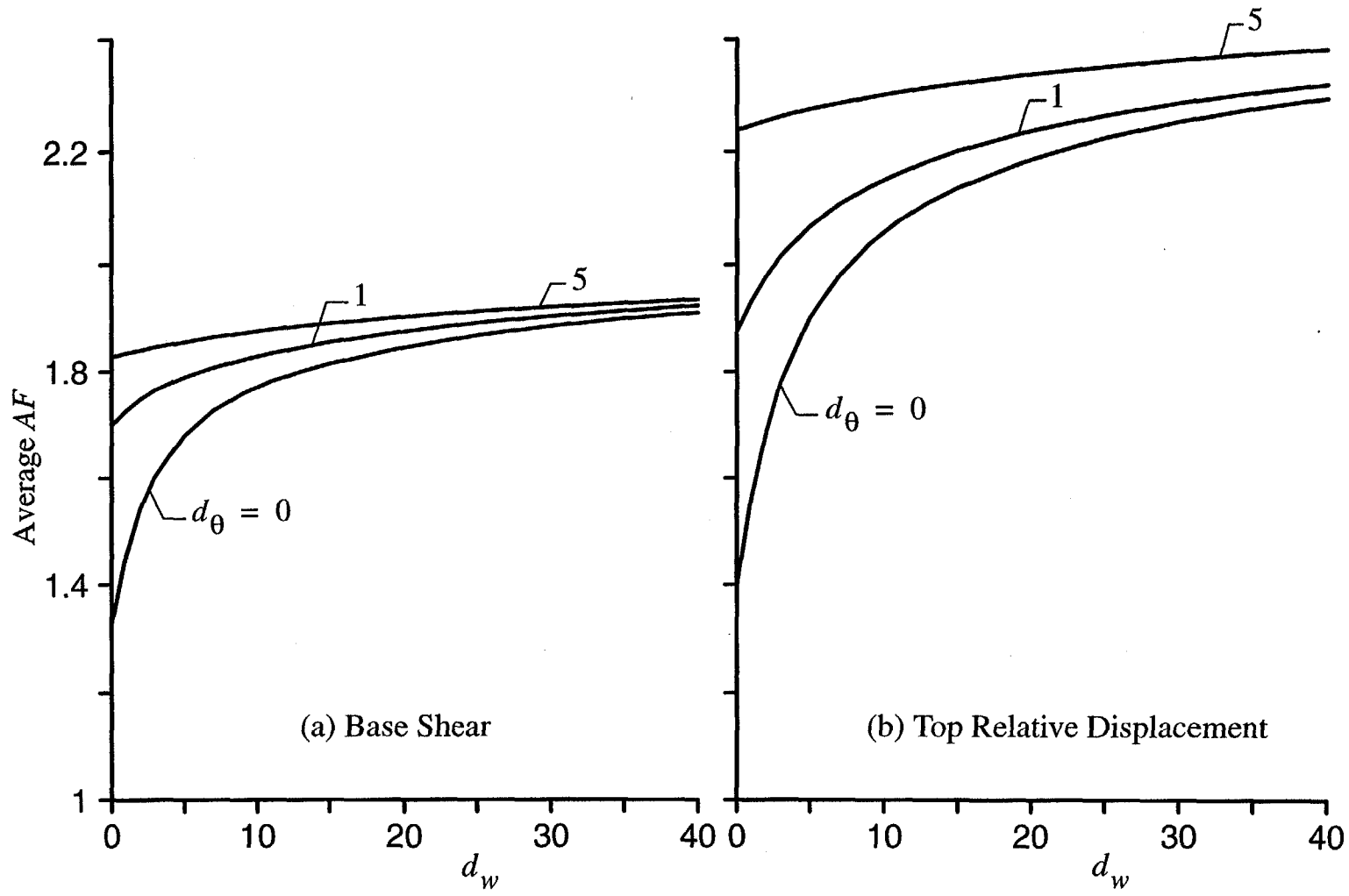

Fig. 6.3 Amplification Factors for Base Shear and Top Relative Displacement Averaged over Period Range $T_1 = 0.1$ to 0.5 sec for Systems Subjected to El Centro Earthquake Record ($\nu = 1/3$, $\delta = 0.1$, $\mu_w = 0$, $\delta_w = 0.04$).

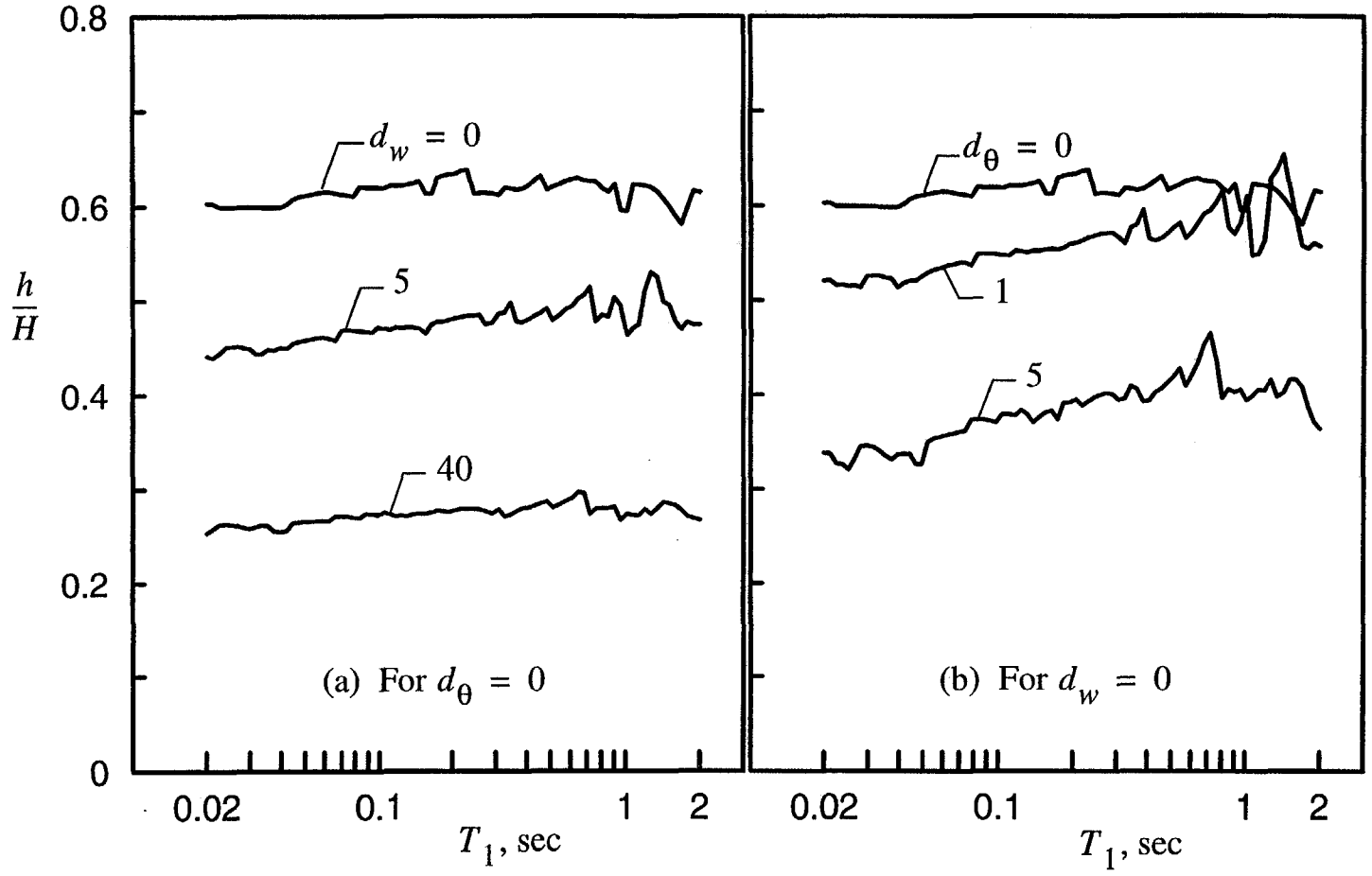

Fig. 6.4 Normalized Effective Heights for Systems with Different Wall and Base Flexibilities Subjected to El Centro Earthquake Record ($\nu = 1/3$, $\delta = 0.1$, $\mu_w = 0$, $\delta_w = 0.04$).

SECTION 7
LIMITATIONS OF SOLUTIONS

The information presented in the preceding sections is limited by the assumption of complete bonding between the wall and retained medium which makes possible the development of negative or tensile normal pressures on the wall. Of special interest in this regard are the tensile pressures developed near the top (see Fig. 4.1) when the pressures for the remainder of the wall, like those induced by gravity forces, are compressive. For ground-motion intensities for which the tensile pressures exceed the gravity-induced compressive pressures, the backfill will naturally separate from the wall, and this separation will increase the wall shears and bending moments over the levels computed on the assumption of complete bonding.

The information presented is also limited by the assumption of uniform properties for the retained medium. In reality, the shear modulus of the medium is likely to increase with depth, and this variation will affect both the magnitudes and distributions of the wall pressures and associated forces. For a rigid wall that is rotationally constrained at the base and for a medium for which the shear modulus increases parabolically from zero at the top to a maximum at the base, it has been shown (Veletsos and Younan, 1994b) that the wall pressure induced by ground shaking vanishes at the top, and that the resulting wall forces are smaller than those obtained for a uniform medium with a shear modulus equal to the mean value of the varying modulus. Similar results also are expected for the more general system examined here. It is concluded that, being of opposite signs, the separation effects at the wall-medium interface and the effects of vertical variability in the shear modulus for the medium will tend to compensate each other.

A measure of these effects is provided in Fig. 7.1, in which the static values of the base shear $(V_b)_{st}$ and base moment $(M_b)_{st}$ in rotationally constrained rigid walls are compared for the following three cases: (1) a uniform stratum with complete bonding to the wall, i.e., the conditions considered in the present study; (2) a uniform stratum with no tensile resistance at its interface with the wall; and (3) a fully bonded stratum for which the shear modulus $G(\eta)$ increases from top to bottom according to

$$G(\eta) = G_o(1-\eta^2) \tag{7}$$

where G_o = its base or maximum value. The results are plotted as a function of the flexibility factor d_θ, in which the shear modulus for the nonuniform medium is taken equal to its average value G_{av}.

In evaluating the separation effects at the wall-medium interface, the gravity-induced wall pressures are computed for a friction angle for the soil $\phi = 30°$, the pressures due to the ground shaking are computed for a maximum ground acceleration $\ddot{X}_g = 0.3g$, and the dynamic tensile pressures near the top are neglected when they exceed the gravity-induced pressures.

In addition to confirming the anticipated interrelationships, the information in Fig. 7.1 emphasizes the need for further studies regarding the effects of both debonding and nonuniformity in material properties.

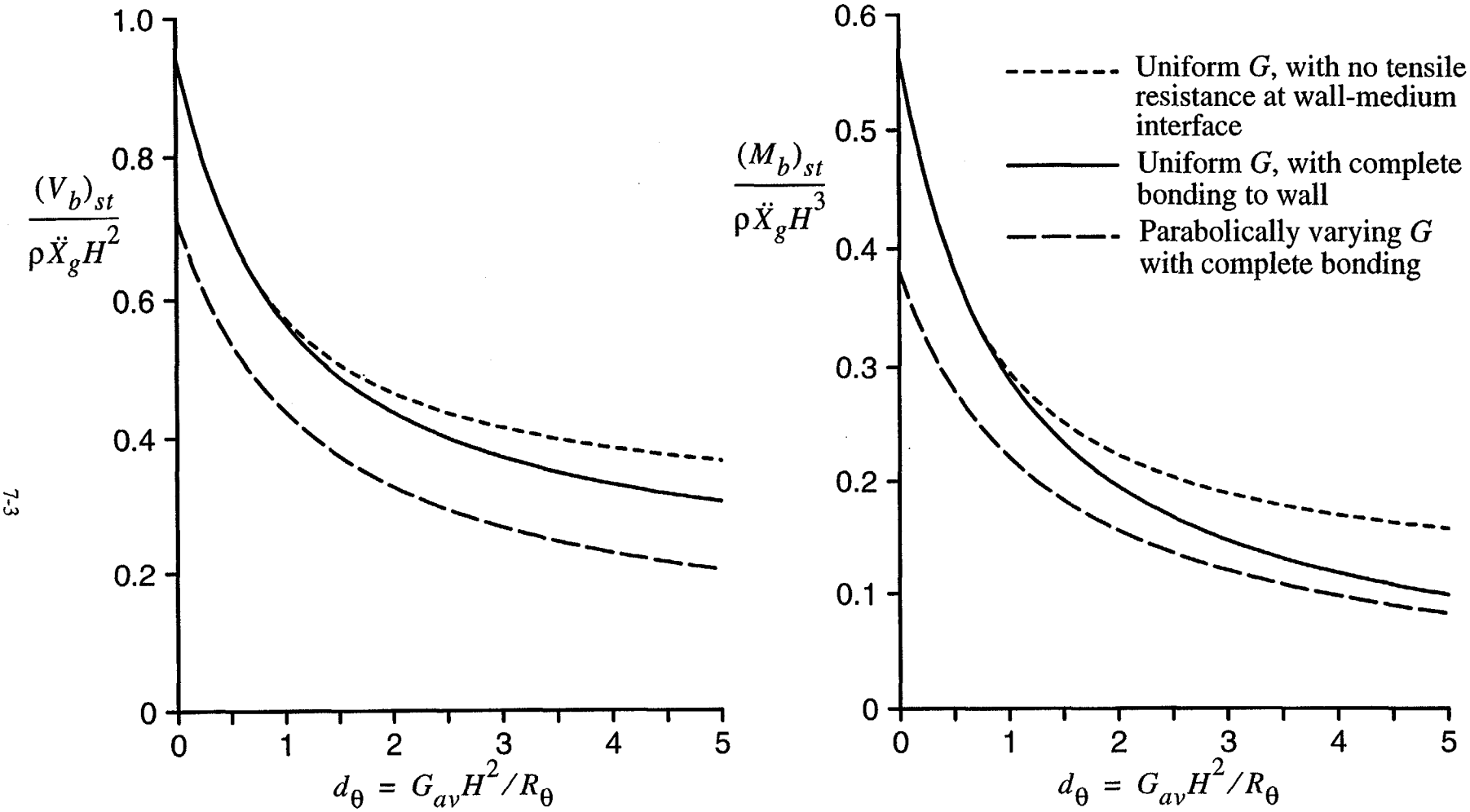

Fig. 7.1 Comparison of Base Shear and Base Moment for Statically Excited Systems with Three Different Backfill Conditions ($\nu = 1/3$, $\mu_w = 0$).

SECTION 8

CONCLUSIONS

Following are some of the more important conclusions of this study.

1. For the soil-wall system examined, both the magnitudes and distributions of the wall displacements, wall pressures and associated forces induced by horizontal ground shaking are quite sensitive to the flexibilities of the wall and its base. Increasing either flexibility reduces the horizontal extensional stiffness of the retained medium relative to its shearing stiffness, and this reduction decreases the proportion of the soil inertia forces that gets transferred to the wall and, hence, the forces developed in it.

2. For realistic wall flexibilities, the total wall force or base shear is one-half or less of that obtained for a fixed-based, rigid wall, and the corresponding reduction in the overturning base moment is even larger. With the information that has been presented, the precise dependence of these critical forces on the flexibilities of the wall and its base may be evaluated readily.

3. When the dynamic amplification effects of the retained medium are neglected, the magnitude of the total wall force obtained for realistic wall flexibilities by the present method of analysis is in reasonable agreement with that computed by the limit-state, Mononobe-Okabe method which also disregards the dynamic amplifications. Additionally, the effective wall height, which is the height by which the total wall force must be multiplied to obtain the overturning base moment, may well be of the order of 40 percent or less of the actual wall height. These values are in close agreement with the 1/3 value involved in the original M-O method, and substantially smaller than the 60 percent value recommended in the Seed-Whitman modification of the method.

4. For systems excited by earthquake ground motions of the type recorded during the El Centro, California event, the dynamic amplification factor for total wall force for the most unfavorable combination of system parameters is likely to vary from 1.3 for fixed-based, rigid walls to 1.9 for walls of high flexibility. The effective wall height, on the other hand, is insensitive to the ground motion characteristics, and may be taken equal to that obtained for 'statically excited' systems.

5. Even for the 1940 El Centro earthquake motion, the maximum wall displacement relative to the moving base for realistic systems is found to be less than the values of 0.1% to 0.4% of the wall height normally accepted as the minimum required to develop a limit state in the retained material.

6. The comprehensive numerical solutions presented and their analysis provide not only valuable insights into the effects and relative importance of the numerous factors that influence the response of the systems examined, but also a sound framework for assessing the behavior of even more complex soil-wall systems. It is hoped that the information presented will also lead to a greater appreciation than appears to exist at present of the value of elastic methods of analysis for the problem examined.

7. The effects of nonuniformity in the shear modulus of the retained medium and of separation at the wall-medium interface were examined briefly from a static point of view. The dynamic aspects of these issues require further study.

SECTION 9

REFERENCES

ATC (1981). *Seismic design guidelines for highway bridges*. Applied Technology Council, Report No. ATC-6, Palo Alto, California.

Andersen, G. R., Whitman, R. V., and Germaine, J. T. (1987). "Tilting response of centrifuge-modeled gravity retaining wall to seismic shaking: description of tests and initial analysis of results," *Report R87-14*, Department of Civil Engrg., MIT, Cambridge, MA.

Arias, A., Sanchez-Sesma, F. J., and Ovando-Shelley, E. (1981). "A simplified elastic model for seismic analysis of earth-retaining structures with limited displacements." *Proc. Int. Conf. on Recent Adv. in Geotech. Earthquake Engrg. and Soil Dyn.*, University of Missouri, Rolla, MO, I, 635-642.

Clough, R. W., and Penzien, J. (1994). *Dynamics of Structures*. McGraw Hill, New York, NY, pp. 344-351.

Clough, G. W., and Duncan, J. M. (1990). "Earth pressures." *Foundation Engineering Handbook*, Edited by H. Y. Fang, Chapman & Hall, New York, NY, pp. 223-235.

Felgar, R. P. (1950). "Formulas for integrals containing characteristic functions of a vibrating beam." *Circular No. 14*, Bureau of Engineering Research, The University of Texas, Austin, Texas.

Finn, W. D. Liam, Yogendrakumar, M., Otsu, H., and Steedman, R. S. (1989). "Seismic response of a cantilever retaining wall: centrifuge model test and dynamic analysis." *Proc. Fourth Int. Conf. on Soil Dyn. and Earthquake Engrg.,* Computational Mechanics Publications, Southampton, pp. 331-431.

Matuo, H., and Ohara, S. (1960). "Lateral earth pressure and stability of quay walls during earthquakes." *Proc. 2nd World Conf. Earthquake Engrg.*, International Association for Earthquake Engineering, Tokyo, Japan.

Mononobe, N., and Matuo, H. (1929). "On the determination of earth pressures during earthquakes." *Proc. World Engrg. Congress,* Tokyo, Japan, Vol. 9.

Nazarian, H. N., and Hadjian, A. H. (1979). "Earthquake-induced lateral soil pressures on structures." *J. of the Geotech. Engrg. Div.*, ASCE, 105(9), 1049-1066.

Nadim, F., and Whitman, R. V. (1983). "Seismically induced movement of retaining walls." *J. of Geotech. Engrg.*, ASCE, 109(7), 915-931.

Okabe, S. (1924). "General theory of earth pressure and seismic stability of retaining wall and dam." *J. Japan Soc. Civil Engrs.*, Tokyo, Japan, 12(1).

Pais A., and Kausel, E. (1988). "Approximate formulas for dynamic stiffnesses of rigid foundations." *Soil Dyn. & Earthquake Engrg.*, 7(4), 213-227.

Prakash, S. (1981). "Analysis of rigid retaining walls during earthquakes." *Proc. Int. Conf. on Recent Adv. in Geotech. Earthquake Engrg. and Soil Dyn.*, University of Missouri, Rolla, MO., Vol. III, pp. 1-28.

Richards, J. and Elms, D. G. (1979). "Seismic behavior of gravity retaining walls." *J. Geotech. Engrg. Div.*, ASCE, 105(4), 449-464.

Roesset, J. M., Whitman, R. V., and Dobry, R. (1973). "Modal analysis for structures with foundation interaction." *J. Struct. Div.*, ASCE, 99(3), 399-416.

Seed, H. B., and Whitman, R. V. (1970). "Design of earth retaining structures for dynamic loads." *Proc. Speciality Conf. on Lateral Stresses in the Ground and Design of Earth Retaining Structures,* ASCE, pp. 103-147.

Siller, T. J., Christiano, P. P., and Bielak, J. (1991). "Seismic response of tied-back retaining walls." *Earthquake Engrg. & Struct. Dyn.*, 20(7), 605-620.

Sun, K. and Lin, G. (1995). "Dynamic response of soil pressure on retaining wall." *Proc. Third Int. Conf. on Recent Advances in Geotech. Earthquake Engrg. and Soil Dyn.*, University of Missouri, Rolla, Mo.,Vol. I, 347-350.

Veletsos, A. S., and Dotson, K. W. (1988). "Horizontal impedances for radially inhomogeneous viscoelastic soil layers." *Earthquake Engrg. & Struct. Dyn.*, 16(7), 947-966.

Veletsos, A. S., and Verbic, B. (1973). "Vibration of viscoelastic foundations." *Earthquake Engrg. & Struct. Dyn.*, 2(4), 87-102.

Veletsos, A. S., and Younan, A. H. (1994a). "Dynamic soil pressures on rigid retaining walls," *Earthquake Engrg. & Struct. Dyn.*, 23(3), 275-301; see also Discussions by Chang, Y. W. and by Wolf, J. P., and Reply by Authors, 24(9), 1283-1293; also available as *Report 52357*, Brookhaven National Laboratory, Upton, N.Y.

Veletsos, A. S., and Younan, A. H. (1994b). "Dynamic modeling and response of soil-wall systems." *J. of Geotech. Engrg.*, ASCE, 120(12), 2155-2179; also available as *Report 52402*, Brookhaven National Laboratory, Upton, N.Y.

Veletsos, A. S., and Younan, A. H. (1995). "Dynamic soil pressures on vertical walls," State-of-the-art paper, *Proc. Third Int. Conf. on Recent Adv. in Geotech. Earthquake Engrg. and Soil Dyn.*, University of Missouri, Rolla, MO, III, 1589-1604.

Whitman, R. V. (1990). "Seismic design and behavior of gravity retaining walls." *Proc. Specialty Conf. on Design & Construction of Earth Retaining Structures*, ASCE, pp. 817-842.

Whitman, R. V. (1991). "Seismic design of earth retaining structures." *Proc. 2nd Int. Conf. on Recent Adv. in Geotech. Earthquake Engrg. and Soil Dyn.*, University of Missouri, Rolla, MO., Vol. II, pp. 1767-1777.

Wood, J. H. (1973). "Earthquake-induced soil pressures on structures." *Report EERL 73-05*, Earthquake Engineering Research Laboratory, California Institute of Technology, Pasadena, CA.

SECTION 10

APPENDIX: EQUATIONS OF MOTION

Unlike the sign convention for wall pressures and displacements used in the body of this paper, the sign convention used in this Appendix is that used in theory of elasticity. Specifically, normal pressures are considered to be positive when tensile, and horizontal displacements are positive when directed along the positive x-axis.

It is convenient to rewrite (1) in the form

$$w(\eta, t) = \sum_{j=0}^{J} \phi_j(\eta)\, q_j(t) \tag{8}$$

where $\phi_0(\eta) = \eta$ and $q_0(t) = H\theta(t)$. For a harmonic base motion with an acceleration

$$\ddot{x}_g(t) = \ddot{X}_g e^{i\omega t} \tag{9}$$

the generalized coordinates $q_j(t)$ are of the form

$$q_j(t) = Q_j e^{i\omega t} \tag{10}$$

where Q_j are their amplitudes. The equations of motion for the system may then be written as

$$(\mathbf{S} - \omega^2\mathbf{M})\mathbf{Q} = -\rho\ddot{X}_g H^2 \mathbf{A} \tag{11}$$

where $\mathbf{M}$ = a $(J+1)\times(J+1)$ mass matrix defined by

$$\mathbf{M} = \mu_w H \begin{bmatrix} 1/3 & \langle\eta, \phi_1\rangle & \langle\eta, \phi_2\rangle & \cdots & \langle\eta, \phi_J\rangle \\ \langle\eta, \phi_1\rangle & 1 & 0 & \cdots & 0 \\ \langle\eta, \phi_2\rangle & 0 & 1 & \cdots & 0 \\ \cdots & \cdots & \cdots & \cdots & \cdots \\ \langle\eta, \phi_J\rangle & 0 & 0 & \cdots & 1 \end{bmatrix} \tag{12}$$

and $\mathbf{S}$ = a stiffness matrix of the same size. The latter matrix may conveniently be expressed as the sum of a diagonal matrix $\mathbf{S_o}$, defined by

$$\mathbf{S}_o = \frac{D_w^*}{H^3}\begin{bmatrix} \frac{R_\theta H}{D_w} & 0 & 0 & \cdots & 0 \\ 0 & \lambda_1^4 & 0 & \cdots & 0 \\ 0 & 0 & \lambda_2^4 & \cdots & 0 \\ \cdots & \cdots & \cdots & \cdots & \cdots \\ 0 & 0 & 0 & \cdots & \lambda_J^4 \end{bmatrix} \tag{13}$$

where $D_w^* = D_w(1 + i\delta_w)$, and a fully populated matrix $\mathbf{S_i}$ with elements

$$(S_i)_{jk} = H \sum_{n=1}^{N} \frac{\langle \phi_j, \psi_n \rangle \langle \phi_k, \psi_n \rangle}{\langle \psi_n, \psi_n \rangle} K_n \tag{14}$$

The symbol $\langle a, b \rangle$ in (12) and (14) represents the integral over the interval [0,1] of the product of the bracketed functions, and the factor λ_j in (13) represents the coefficient in the expression for the *j*th circular natural frequency of the uniform cantilever beam

$$\omega_{w,j} = \frac{\lambda_j^2}{H^2}\sqrt{\frac{D_w}{\mu_w}} \tag{15}$$

Additionally, $\mathbf{Q}$ = the vector of the generalized coordinate amplitudes Q_j, and $\mathbf{A}$ = the vector of the normalized exciting forces, the elements of which are

$$A_j = \langle \phi_j, 1 \rangle \frac{\mu_w}{\rho H} - \frac{1}{\rho \ddot{X}_g H} \sum_{n=1}^{N} \langle \phi_j, \psi_n \rangle K_n U_n \tag{16}$$

The expressions for the integrals in (12), (14) and (16) are given later in this Appendix. The quantity K_n in (14) and (16), which represents the complex-valued impedance or dynamic stiffness of the medium between the wall and the far field when they are both vibrating in the *n*th shear-beam mode $\psi_n(\eta)$, is given by (Veletsos and Younan, 1994b)

$$K_n = \frac{(2n-1)\pi}{2}\sqrt{\frac{2}{1-\nu}}\frac{G}{H}\sqrt{(1+i\delta)[1-(\omega/\omega_n)^2 + i\delta]} \tag{17}$$

where ω_n = the nth circular natural frequency of the shear-beam, defined by

$$\omega_n = \frac{(2n-1)\pi}{2}\frac{v_s}{H} \tag{18}$$

Finally, U_n in (16) represents the amplitude of the nth term in a modal expansion of the displacement of the medium at the far field, and it is given by

$$U_n = -\frac{16}{\pi^3}\frac{\rho \ddot{X}_g H^2}{G}\frac{1}{(2n-1)^3}\frac{1}{1-(\omega/\omega_n)^2 + i\delta} \tag{19}$$

With the vector **Q** determined from the solution of the system of algebraic equations (11), the generalized coordinates q_j are determined from (10), the relative wall displacements are determined from (1) or (8), and the wall pressures are computed from

$$\sigma(\eta, t) = \sum_{n=1}^{N} K_n \left\{ U_n - \sum_{j=0}^{J} \frac{\langle \phi_j, \psi_n \rangle}{\langle \psi_n, \psi_n \rangle} Q_j \right\} \psi_n(\eta)\, e^{i\omega t} \tag{20}$$

Finally, the shear and bending moment at the wall base are computed either by appropriate integrations of the pressures and inertia forces acting on the wall as

$$\begin{aligned} V_b(t) &= H\langle \sigma, 1 \rangle - \mu_w H \ddot{x}_g(t) - \mu_w H \langle \ddot{w}, 1 \rangle \\ &= H \sum_{n=1}^{N} K_n \left\{ U_n - \sum_{j=0}^{J} \frac{\langle \phi_j, \psi_n \rangle}{\langle \psi_n, \psi_n \rangle} Q_j \right\} \langle \psi_n, 1 \rangle\, e^{i\omega t} \\ &\quad - \mu_w \ddot{X}_g H e^{i\omega t} + \omega^2 \mu_w H \sum_{j=0}^{J} \langle \phi_j, 1 \rangle Q_j e^{i\omega t} \end{aligned} \tag{21}$$

$$\begin{aligned} M_b(t) &= H^2\langle \sigma, \eta \rangle - \frac{1}{2}\mu_w H^2 \ddot{x}_g(t) - \mu_w H^2 \langle \ddot{w}, \eta \rangle \\ &= H^2 \sum_{n=1}^{N} K_n \left\{ U_n - \sum_{j=0}^{J} \frac{\langle \phi_j, \psi_n \rangle}{\langle \psi_n, \psi_n \rangle} Q_j \right\} \langle \psi_n, \eta \rangle\, e^{i\omega t} \\ &\quad - \frac{1}{2}\mu_w \ddot{X}_g H^2 e^{i\omega t} + \omega^2 \mu_w H^2 \sum_{j=0}^{J} \langle \phi_j, \eta \rangle Q_j e^{i\omega t} \end{aligned} \tag{22}$$

or by appropriate differentiations of the wall displacement as

$$V_b(t) = -\frac{D_w^*}{H^3} w'''|_{\eta=0} = \frac{2D_w^*}{H^3} \sum_{j=1}^{J} \alpha_j \lambda_j^3 Q_j e^{i\omega t} \tag{23}$$

$$M_b(t) = -\frac{D_w^*}{H^2} w''|_{\eta=0} = -\frac{2D_w^*}{H^2} \sum_{j=1}^{J} \lambda_j^2 Q_j e^{i\omega t} \tag{24}$$

where a dot superscript denotes differentiation with respect to t while a prime superscript denotes differentiation with respect to η. The former expressions converge more rapidly than the latter and were used in the numerical evaluations. The base moment can also be determined from

$$M_b(t) = R_\theta^* w'|_{\eta=0} = R_\theta^* Q_o e^{i\omega t} \tag{25}$$

where $R_\theta^* = R_\theta(1 + i\delta_w)$. The rate of convergence of this expression is the same as that of (22). Good convergence is normally achieved with as few as five beam modes or a total of six terms in (8).

The natural modes of the fixed-based cantilever beam, $\phi_j(\eta)$ for $j \geq 1$, are given by

$$\phi_j(\eta) = \cosh\lambda_j\eta - \cos\lambda_j\eta - \alpha_j(\sinh\lambda_j\eta - \sin\lambda_j\eta) \tag{26}$$

where

$$\alpha_j = \frac{\sinh\lambda_j - \sin\lambda_j}{\cosh\lambda_j + \cos\lambda_j} \tag{27}$$

and the expressions for the various integrals in the equations presented are

$$\langle\psi_n, 1\rangle = \frac{2}{\pi}\frac{1}{(2n-1)} \tag{28}$$

$$\langle\psi_n, \eta\rangle = \frac{4}{\pi^2}\frac{(-1)^{n+1}}{(2n-1)^2} \tag{29}$$

$$\langle\psi_n, \psi_n\rangle = 0.5 \tag{30}$$

$$\langle\phi_j, 1\rangle = \begin{cases} j = 0 & 0.5 \\ j \neq 0 & \dfrac{2\alpha_j}{\lambda_j} \end{cases} \tag{31}$$

$$\langle\phi_j, \eta\rangle = \begin{cases} j = 0 & 1/3 \\ j \neq 0 & \dfrac{2}{\lambda_j^2} \end{cases} \tag{32}$$

$$\langle\phi_j, \psi_n\rangle = \begin{cases} j = 0 & \dfrac{4}{\pi^2}\dfrac{(-1)^{n+1}}{(2n-1)^2} \\ j \neq 0 & \dfrac{2\lambda_j\varepsilon_n[\lambda_j - (-1)^{j+n}\alpha_j\varepsilon_n]}{\lambda_j^4 - \varepsilon_n^4} \end{cases} \tag{33}$$

where $\varepsilon_n = (2n-1)\pi/2$. The integrals in (31) and (32) for $j \neq 0$ are given in Felgar (1950), while all the other were derived from basic principles.